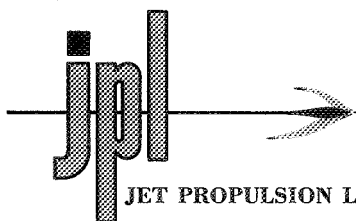NATIONAL AERONAUTICS AND SPACE ADMINISTRATION

Technical Report 32-1489

Effect of Elastic End Rings on the Eigenfrequencies of Finite Length Thin Cylindrical Shells

Michel El Raheb

JET PROPULSION LABORATORY
CALIFORNIA INSTITUTE OF TECHNOLOGY
PASADENA, CALIFORNIA

March 1, 1971

April 15, 1971

Recipients of Jet Propulsion Laboratory
Technical Report 32-1489

N71-20516

Subject: Errata

Gentlemen:

Please note the following corrections to Technical Report 32-1489, <u>Effect of Elastic End Rings on the Eigenfrequencies of Finite Length Thin Cylindrical Shells</u>, by Michel El Rehab, dated March 1, 1971:

(1) On page 3, last line of Eq. (3):

$$k_{x\theta} = + \frac{\partial^2 w}{\partial x \partial \theta}$$

(2) On page 5, last block of Table 2:

	rn^2	$1.0 + 2\nu^2 + rn^2$	2	2	4
	$1.0 + 2\nu^2 + rn^2$	$\left(\frac{1-\nu}{2}\right)^{1/2} n$	2	6	
≥ 3	$\left(\frac{1-\nu}{2}\right)^{1/2} n$	$(n^2 + 1)^{1/2}$	4	4	
	$(n^2 + 1)^{1/2}$		6	2	

(3) On page 7, Eq. (17):

$$\left[M_{T,ij}\right]\begin{Bmatrix} w_n(\ell/2) \\ u_n(\ell/2) \\ v_n(\ell/2) \\ w'_n(\ell/2) \end{Bmatrix} = \left[M_{d,ij}\right]\begin{Bmatrix} \tilde{q}_{xx}(\ell/2) \\ \tilde{n}_{xx}(\ell/2) \\ \tilde{n}_{x\theta}(\ell/2) \\ \tilde{m}_{xx}(\ell/2) \end{Bmatrix} \tag{17}$$

(4) On page 8, next-to-last sentence in column 2 (text corrections are underscored):

For low circumferential wave number with n = 2, n = 3, and n = 4, the $\tilde{\omega}_{LF}$ corresponding to the first seven modes was plotted against S_{tx} and W_r as shown in Figs. 6-8 for the H-type section only.

(5) On page 9, Fig. 7, horizontal grid line at 0.5 should read "FIRST MODE" instead of "FOURTH MODE".

(6) On page 10, last sentence under Section IV-B:

After some range of S_{tx}, $\tilde{\omega}_{s,3}$ changes asymptote to the second frequency of FX2/FX2 in Region II.
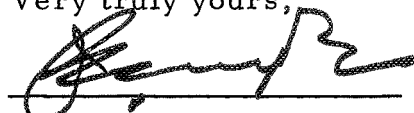
(7) On page 10, last sentence in second paragraph under Section IV-C:

This implies that crossing of the five lines representing the first five system eigenfrequencies is impossible.
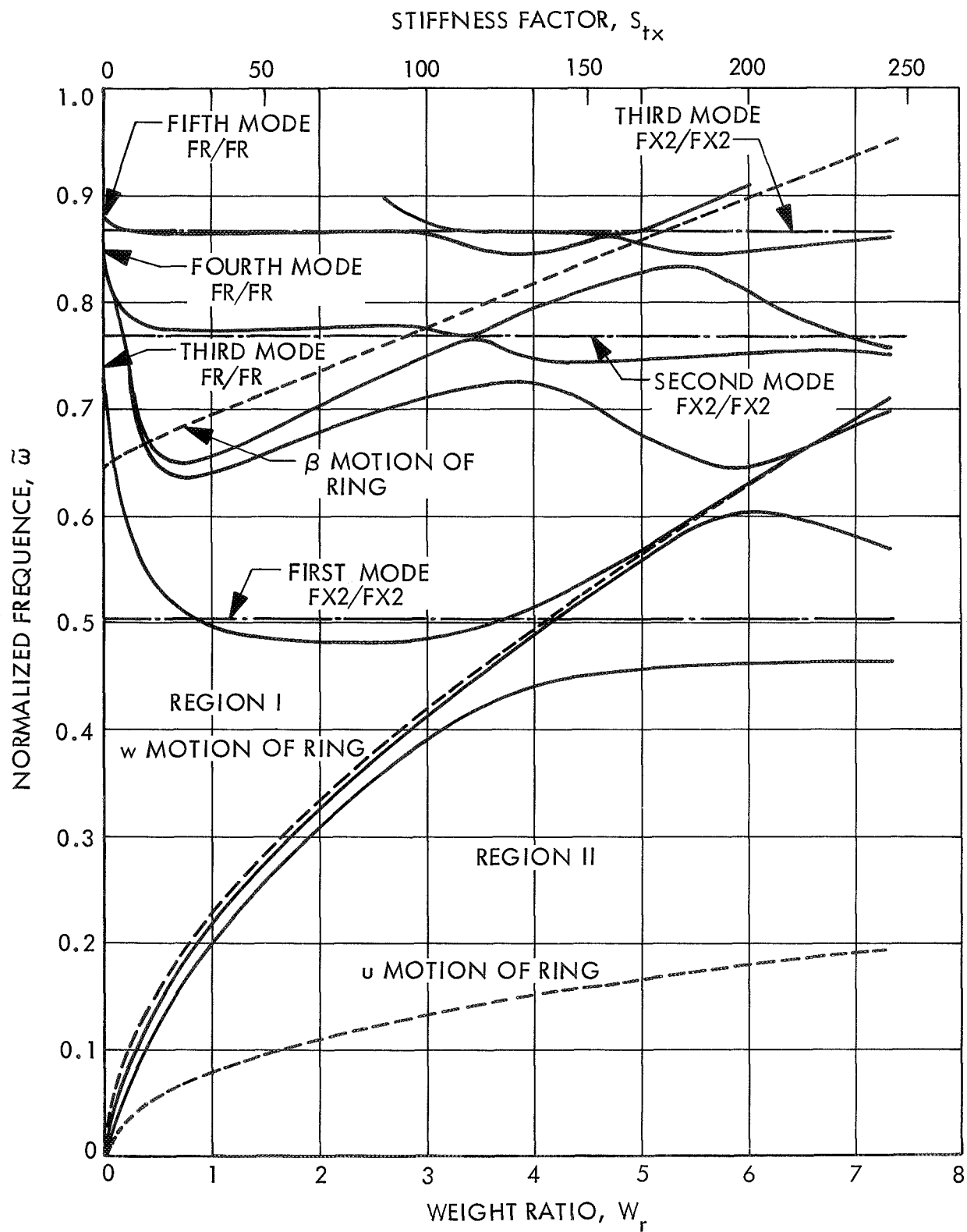
(8) On page 18, equation on next-to-last line:

$$C_n(4) = r^2 n^2 \left(-4n^4 + \frac{3(3-\nu)}{(1-\nu)}\tilde{\omega}^2 n^2 - \frac{4\tilde{\omega}^4}{(1-\nu)}\right)$$

$$+ \omega\left[2n^2 - \frac{3-\nu}{1-\nu}\tilde{\omega}^2 + 3 + 2\nu\right]$$

Very truly yours,

John Kempton, Manager
Publications Section

2

NATIONAL AERONAUTICS AND SPACE ADMINISTRATION

Technical Report 32-1489

Effect of Elastic End Rings on the Eigenfrequencies of Finite Length Thin Cylindrical Shells

Michel El Raheb

Preface

The work described in this report was performed by the Engineering Mechanics Division of the Jet Propulsion Laboratory.

Contents

Tables

Contents (contd)

Figures

Abstract

The effect of elastic end rings on the eigenfrequencies of thin cylindrical shells was studied by using an exact solution of the linear eigenvalue problem. The in-plane boundary conditions which proved to be very influential in the neighborhood of the minimum frequency were exactly satisfied. The out-of-plane and torsional rigidities of the ring were found to govern the overall shell stiffness. Considerable mode interaction was noticed at low circumferential wave numbers for low values of the ring stiffness.

Rings with closed section were found to be more efficient than those with open section for the same values of weight ratio. No appreciable difference was noticed between rings fixed from the inside or the outside of the shell mid-surface.

Effect of Elastic End Rings on the Eigenfrequencies
of Finite Length Thin Cylindrical Shells

I. Introduction

The linear and nonlinear response to external loading of shells of revolution has been studied previously without much consideration of the boundary conditions (Ref. 1). Most of the work was carried out for infinitely long shells with no account of the boundary effect. The classical simply supported boundary condition at both ends SS1/SS1 was also assumed. It is thus of interest to find how close these approximate calculations are to some exact analysis which includes the effect of more realistic boundary conditions.

Before going into the complicated problem of the response, the boundary effect is at first studied on the small amplitude low eigenfrequencies of a cylindrical shell. This gives an estimate of the effect of boundary conditions on the linear response problem, since the low eigenfrequencies enter in the evaluation of the generalized coordinates when an eigenfunction expansion type solution is assumed. Previous work in this subject was done by Arnold and Warburton (Refs. 2 and 3), and by Weingarten (Ref. 4), but their analyses were approximate. Forsberg (Refs. 5 and 6) used the same technique as in this work, to obtain an exact solution of the equations of motion. He considered the effect of natural boundary conditions on the low frequency spectrum envelope (i.e., the minimum frequency for all modes with one axial half wave) without giving in-

sight to the effect for other modes, and the range of circumferential and axial wave numbers for which this effect is noticeable.

Total fixity as well as classical simple supports are scarcely found in practical applications. An intermediate state with elastic supports is more commonly encountered. A classical example is a shell with elastic rings at the ends.

The effect of the ring elasticity on the static buckling load of cylindrical shells was studied by Cohen (Ref. 7). He assumed a hypothetical ring with no out-of-plane stiffness and concluded that total fixity could be realized when the stiffness factor $S_t = 2EI_{yy}/Dl^*$ reached the optimum value of 90.5, where I_{yy} was the in-plane moment of inertia of the ring cross section.[1] Such an analysis is inconsistent when applied to dynamics since, as shown in Ref. 8, the in-plane boundary conditions of the shell are the most effective. Therefore, the out-of-plane stiffness of the ring cannot be neglected. Forsberg et al. (Ref. 9) noticed a discrepancy between the calculated frequencies of a cylindrical shell with elastic rings and the frequencies determined experimentally, at low circumferential wave number, when his calculations were based on the assumption that the shell was totally fixed at both ends. However, no further

---

[1] E, D and l^* are defined in the nomenclature.

study was done concerning the boundary effect due to the ring elasticity or the stiffness required to reach a state of total fixity.

In this report, the effect is studied of the ring elasticity on a cylindrical shell with elastic rings at both ends. In the limit, as the ring stiffness goes to zero, the shell approaches the free-free condition. Also, as the ring stiffness goes to very large values, the shell reaches the condition of total fixity. Thus the above two limiting conditions constitute the lower and upper bounds respectively of the boundary condition in question. The ring cross sections were taken to be symmetric open and closed thin sections as well as solid closed sections. These sections were chosen since one can study the effect of eccentricity between the loading point and the center of gravity of the section, on the rigidity and efficiency of the ring. Such eccentricity induces a radial as well as an axial displacement when the section rotates in torsion about an axis normal to its plane. The axial displacement is responsible for the change in the in-plane boundary conditions of the shell. The symmetry of the section also enables the uncoupling of the in-plane and out-of-plane motions of the ring. One could also investigate the effects of the form of the section on its efficiency. The ring fixity position with respect to the shell centerline is also considered.

Due to the number of ring geometrical parameters involved, a detailed analysis of the effect of each parameter is rather impossible. As an alternative, all geometrical parameters are fixed with the exception of the thickness ratio $\tilde{h}$ (thickness of ring/thickness of shell) for each cross section. The increase in shell stiffness resulting from an increase in $\tilde{h}$ can now be studied by looking at the increase in the eigenfrequencies corresponding to a particular mode shape.

The analysis will cover a range of frequencies with mode shapes having twenty or less full waves in the circumferential direction and six or less half waves in the axial direction. This is the range of interest for response modes resulting from smoothly varying external loads.

II. Governing Equations and Exact Solution for any Boundary Condition

A. Method of Comparison

The classical simply supported boundary condition SS1/SS1, as defined in Table 1, will be taken as a basis for comparison. For some boundary condition and for a particular mode shape, i.e., for some m and n, the boundary effect will be measured by looking at the difference between the eigenfrequency with such a boundary condition and the corresponding eigenfrequency of SS1/SS1. A *difference* is now defined as follows:

$$d = \frac{\tilde{\omega}}{\tilde{\omega}_{SS1}} - 1 \text{ (for the same } m \text{ and } n)$$

Table 1. Notation for boundary conditions and motivation

Boundary condition	$u = 0$	$v = 0$	$w = 0$	$w' = 0$	$n_{xx} = 0$	$n_{x\theta} = 0$	$q_{xx} = 0$	$m_{xx} = 0$	Motivation for choice
SS1/SS1 (both ends)		✓	✓		✓			✓	Basis for comparison
SS2/SS2 (both ends)	✓	✓	✓					✓	Effect of axial restraint
SS3/SS3 (both ends)			✓		✓	✓		✓	Effect of circumferential restraint
FX1/FX1 (both ends)		✓	✓	✓	✓				Effect of slope restraint
FX2/FX2 (both ends)	✓	✓	✓	✓					Upper bound for FXR/FXR
FX2/FR	✓	✓	✓	✓	✓	✓	✓	✓	Lower bound for FX2/FXR and effect of free end
FR/FR (both ends)					✓	✓	✓	✓	Lower bound for FXR/FXR
FXR/FXR	Elastic ring at both ends								Effect of elastic ring at both ends

B. Equilibrium and Constitutive Equations

The simplified dynamic equations of equilibrium and the corresponding set of constitutive relations will exclude the following quantities:

(1) In-plane displacements in the curvature relations.

(2) Transverse shear force in the in-plane equilibrium equations.

(3) Order $(h/a)^2$ in the in-plane shear force $n_{x\theta}$ (i.e., $n_{x\theta} \simeq n_{\theta x}$).

(4) Rotary inertia.

These terms were found to have a negligible effect on the eigenfrequencies for finite length thin shells (Ref. 8). In terms of nondimensional quantities, the equilibrium equations and constitutive relations can be written as follows:

$$
\left.\begin{array}{c}
\dfrac{\partial n_{xx}}{\partial x} + \dfrac{\partial n_{x\theta}}{\partial \theta} = \dfrac{\partial^2 u}{\partial \tau^2} \\[2ex]
\dfrac{\partial n_{x\theta}}{\partial x} + \dfrac{\partial n_{\theta\theta}}{\partial \theta} = \dfrac{\partial^2 v}{\partial \tau^2} \\[2ex]
\dfrac{\partial^2 m_{xx}}{\partial x^2} - 2\dfrac{\partial^2 m_{x\theta}}{\partial x\, \partial \theta} + \dfrac{\partial^2 m_{\theta\theta}}{\partial \theta^2} + n_\theta = \dfrac{\partial^2 w}{\partial \tau^2}
\end{array}\right\} \quad (1)
$$

$$
\left.\begin{array}{c}
n_{xx} = \epsilon_{xx} + \nu\epsilon_{\theta\theta} \\[1.5ex]
n_{\theta\theta} = \epsilon_{\theta\theta} + \nu\epsilon_{xx} \\[1.5ex]
n_{x\theta} = \dfrac{1-\nu}{2}\, \epsilon_{x\theta} \\[1.5ex]
n_{\theta x} = n_{x\theta} \\[1.5ex]
m_{xx} = r^2\left(k_{xx} + \nu k_{\theta\theta}\right) \\[1.5ex]
m_{\theta\theta} = r^2\left(k_{\theta\theta} + \nu k_{xx}\right) \\[1.5ex]
m_{x\theta} = r^2\left(1-\nu\right)k_{x\theta} = m_{\theta x} \\[1.5ex]
q_\theta = \dfrac{\partial m_{\theta\theta}}{\partial \theta} - \dfrac{\partial m_{x\theta}}{\partial x}
\end{array}\right\} \quad (2)
$$

The coordinate system and resultant forces and moments are shown in Fig. 1. The geometric parameter r is defined as

$$
r = \frac{h}{(12)^{1/2}\, a}
$$
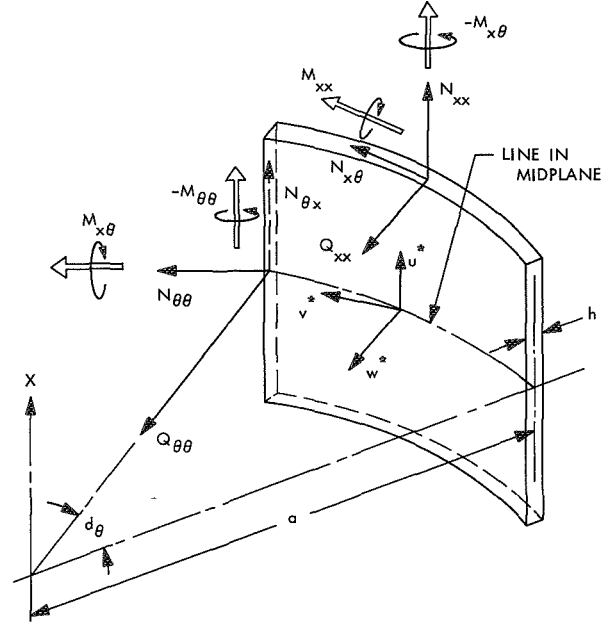
Fig. 1. Element of cylindrical shell

The strain-displacement and nondimensional curvature-displacement relations are given below

$$
\left.\begin{array}{c}
\epsilon_{xx} = \dfrac{\partial u}{\partial x} \\[2ex]
\epsilon_{\theta\theta} = \dfrac{\partial v}{\partial \theta} - w \\[2ex]
\epsilon_{x\theta} = \dfrac{\partial v}{\partial x} + \dfrac{\partial u}{\partial \theta} \\[2ex]
k_{xx} = -\dfrac{\partial^2 w}{\partial x^2} \\[2ex]
k_{\theta\theta} = -\dfrac{\partial^2 w}{\partial \theta^2} \\[2ex]
k_{x\theta} = -\dfrac{\partial^2 w}{\partial x\, \partial \theta}
\end{array}\right\} \quad (3)
$$

Substituting Eqs. (2 and 3) in Eq. (1) we obtain

$$
[D_{ij}]\left\{\begin{array}{c} u \\ v \\ w \end{array}\right\} = 0, \qquad i,j = 1,2,3 \quad (4)
$$

The symmetric matrix of linear differential operators $[D_{ij}]$ is given in Appendix A.

The above operator matrix can be diagonalized in u and v and the resulting uncoupled differential equations for free vibration can be written as follows:

$$
\left.
\begin{aligned}
\mathcal{L}_o\left(u_o\right) &= v\,\frac{dw_o}{dx},\\[2mm]
\mathcal{R}_o\left(w_o\right) &= 0,
\end{aligned}
\right\}
\quad n = 0,
\tag{5}
$$

$$
\left.
\begin{aligned}
\mathcal{L}_n\left(u_n\right) &= \mathcal{S}_{1_n}\left(w_n\right),\\[2mm]
\mathcal{L}_n\left(v_n\right) &= \mathcal{S}_{2_n}\left(w_n\right),\\[2mm]
\mathcal{R}_n\left(w_n\right) &= -\tilde{\omega}^2\,\mathcal{H}_n\left(w_n\right),
\end{aligned}
\right\}
\quad n \geq 1,
\qquad
x \ni \left[-\frac{\ell}{2},\frac{\ell}{2}\right]
\tag{6}
$$

The operators in the above differential equations are linear and ordinary with constant coefficients.[2] Since the above operators are self-adjoint, the solution of the eigenvalue problem in Eqs. (5) and (6) leads to two and three real eigenvalues respectively for each particular eigenfunction. This is similar to the special case of SS1/SS1.

C. Exact Solution of the Differential Equations

The last of Eqs. (5) and (6) admits an exact solution of the form

$$
w_n\left(x\right) = \sum_{j=1}^{j*} A_{nj}\exp\lambda_{nj}x, \quad j^* = 6 \text{ for } n = 0 \text{ and } j^* = 8 \text{ for } n \geq 1
\tag{7}
$$

Upon substitution of Eq. (7) in Eqs. (5) and (6), we obtain the following "characteristic equations" (dispersion relations):

$$
C_o\left(1\right)\lambda_{oj}^6 + C_o\left(2\right)\lambda_{oj}^4 + C_o\left(3\right)\lambda_{oj}^2 + C_o\left(4\right) = 0, \qquad n = 0
$$
$$
C_n\left(1\right)\lambda_{nj}^8 + C_n\left(2\right)\lambda_{nj}^6 + C_n\left(3\right)\lambda_{nj}^4 + C_n\left(4\right)\lambda_{nj}^2 + C_n\left(5\right) = 0, \qquad n \geq 1
\tag{8}
$$

The coefficients $C_o\left(i\right)$ *and* $C_n\left(i\right)$ (function of n, r, ω, v) are given in Appendix C. The type of roots of Eq. (8) changes with $\tilde{\omega}$ and n, as shown in Table 2. The solution of Eqs. (5) and (6) can also be written in the following real form:

$$
\left.
\begin{aligned}
w_n\left(x\right) &= \sum_{j=1}^{j*} B_{nj}\,F_{nj}\left(x\right),\\[2mm]
u_n\left(x\right) &= \mathcal{L}_n^{-1}\left[\mathcal{S}_{1n}\left(w_n\right)\right] = \sum_{j=1}^{j*} B_{nj}G_{nj}\left(x\right),\\[2mm]
v_n\left(x\right) &= \mathcal{L}_n^{-1}\left[\mathcal{S}_{2n}\left(w_n\right)\right] = \sum_{j=1}^{j*} B_{nj}H_{nj}\left(x\right),
\end{aligned}
\right\}
\quad j^* = 6 \text{ for } n = 0 \text{ and } j^* = 8 \text{ for } n \geq 1
\tag{9}
$$

$F_{nj}\left(x\right)$, $G_{nj}\left(x\right)$ and $H_{nj}\left(x\right)$ are real independent functions of x (combinations of trigonometric and hyperbolic functions) which change form with the type of roots of Eq. (8), and B_{nj} are real independent constants of integration. Substituting the expressions given by Eq. (9) in any of the homogeneous boundary conditions of Table 1, leads to a system of homogeneous simultaneous equations in B_{nj}:

$$
\left[\mathcal{S}_{nij}\right]\left\{B_{nj}\right\} = 0,
\qquad
\begin{cases}
i,j = 1 \text{ to } 6, n = 0\\[2mm]
i,j = 1 \text{ to } 8, n \geq 1
\end{cases}
\tag{10}
$$

---

[2]See Eq. (B-5d) of Appendix B.

Table 2. Change of roots of the characteristic equation

n	Range of $\tilde{\omega}$		Type of roots		
	Greater	Less	No. of imaginary	No. of real	No. of complex
0	0	$(1-\nu^2)^{\frac{1}{2}}$	2		4
	$(1-\nu^2)^{\frac{1}{2}}$	1.0	2	4	
	1.0		4	2	
1	0	$\left(\dfrac{1-\nu}{2}\right)^{\frac{1}{2}}$	2	2	4
	$\left(\dfrac{1-\nu}{2}\right)^{\frac{1}{2}}$	0.962	4		4
	0.962	$(n^2+1)^{\frac{1}{2}}$	4	4	
	$(n^2+1)^{\frac{1}{2}}$		6	2	
2	rn^2	0.978	2	2	4
	0.978	$\left(\dfrac{1-\nu}{2}\right)^{\frac{1}{2}}n$	2	6	
	$\left(\dfrac{1-\nu}{2}\right)^{\frac{1}{2}}n$	$(n^2+1)^{\frac{1}{2}}$	4	4	
	$(n^2+1)^{\frac{1}{2}}$		6	2	
$\geqq 3$	rn^2	1.0	2	2	4
	1.0	$\left(\dfrac{1-\nu}{2}\right)^{\frac{1}{2}}n$	2	6	
	$\left(\dfrac{1-\nu}{2}\right)^{\frac{1}{2}}n$	$(n^2+1)^{\frac{1}{2}}$	4	4	
	$(n^2+1)^{\frac{1}{2}}$		6	2	

Equation (10) has a nontrivial solution if and only if

$$\det[\mathscr{G}_{nij}] = 0 \qquad (11)$$

All boundary conditions, except SS1/SS1, lead to an eigen-determinant in Eq. (11) which depends on both geometrical parameters ℓ and r, and which is singular only for values of $\tilde{\omega} = (\tilde{\omega})_{\text{resonance}}$. For the special case of boundary condition SS1/SS1, the eigendeterminant in (11) can be expressed as a product:

$$\det[\mathscr{G}_{nij}] = F_n^*\left(\frac{\ell}{2}\right) \cdot \det[\mathscr{D}_{ij}]$$

$F_n^*(\ell/2)$ is formed of the independent functions $F_{nj}(x)$ given in Eq. (9), evaluated at $x = \ell/2$; and $\det[\mathscr{D}_{ij}]$ is independent of ℓ. The dependence of $\tilde{\omega}$ on ℓ implies that $\det[\mathscr{D}_{ij}]$ cannot vanish at $\tilde{\omega} = (\tilde{\omega})_{\text{resonance}}$. As a consequence, $F_n^*(\ell/2)$ is equal to zero. This gives rise to the well known one-term trigonometric solution for boundary condition SS1/SS1.

The computations of the exact low frequencies and their corresponding eigenvectors and stress field, were performed on a UNIVAC 1108. Figures 2a and 2b show the low frequency spectrum and corresponding per cent difference (%d) for a shell with boundary condition $FX2/FX2$, where

$$\%d = 100\left(\frac{\tilde{\omega}_{\text{boundary condition}}}{\tilde{\omega}_{SS1}} - 1\right)$$

and with $\ell = 1$ and $a/h = 400$. Figure 3 shows the %d for $\ell = 2$. We note that the maximum %d occurs in the neighborhood of the minimum frequency. The difference d is large even for axial wave numbers greater than 1. The range of circumferential wave number n for which the in-plane boundary conditions are influential decreases with the increase of the nondimensional axial wavelength ℓ/m and the thickness ratio h/a, although the maximum difference d increases with the increase of ℓ/m and a/h.
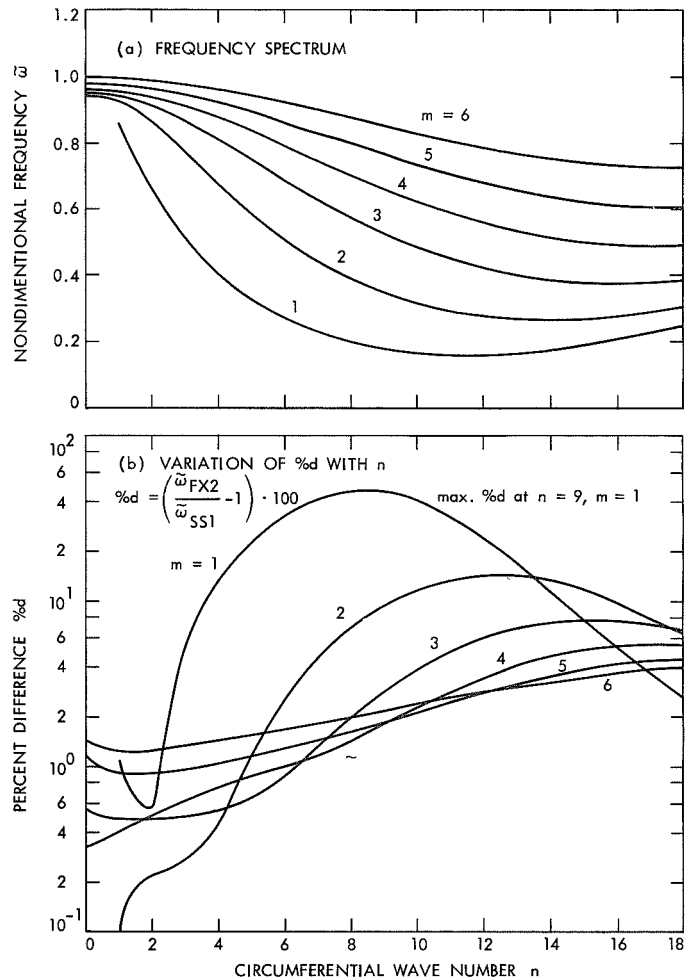

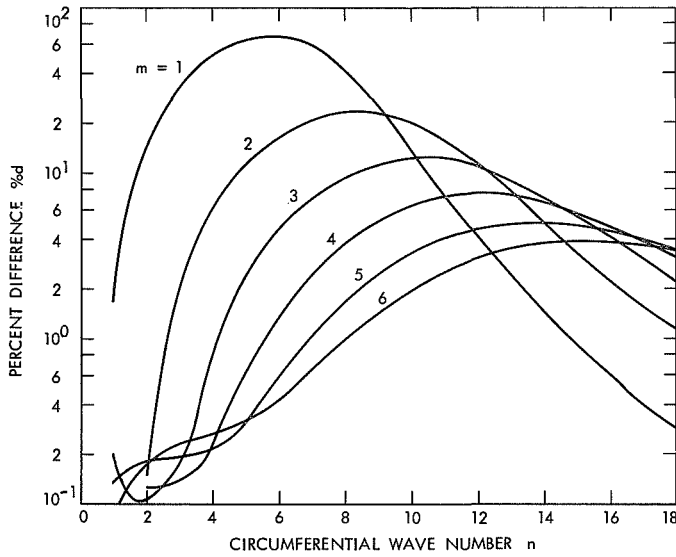Fig. 2. Boundary condition FX2/FX2, $\ell = 1$, $a/h = 400$

Fig. 3. Variation of %d with n for boundary
condition FX2/FX2, $\ell = 2$, $a/h = 400$

Fig. 4. Element of stiffening ring

The %d decreases with m for small n and the effect is reversed for large n.

The steps necessary to find the eigenvalues and eigenfunctions are as follows. First the frequency is assumed. The characteristic Eq. (8) is solved numerically to find the eight roots (for $n \geq 1$) or six roots (for $n = 0$). Depending on the type of the roots (see Table 2), the form of the solution is determined. Next the coefficients of the eigendeterminant are calculated and its value found. The frequency is then increased by a predetermined amount and the procedure is repeated to find the new value of the eigendeterminant. A change of sign of the eigendeterminant indicates that an eigenfrequency lies between the two assumed frequencies. An iterative procedure is then used to obtain the exact eigenfrequency to any degree of accuracy (taken as 10^{-8}). Once the eigenfrequency has been determined, the eigenvector is found by solving a set of linear simultaneous equations.

III. Equations of Motion and Exact Solution for Boundaries Fixed to Flexible Rings

The effectiveness of the ring as a flexible boundary will be measured by comparing the low frequencies corresponding to boundary condition FXR/FXR to those of $FX2/FX2$ for the same mode shape, i.e., for the same m and n. A difference is now defined as

$$d_f = \frac{\widetilde{\omega}_{fxr}}{\widetilde{\omega}_{fx2}} - 1$$

The difference d_f gives a quantitative measure of how close the boundary with the ring is to its upper bound, the totally fixed case. The stiffness of the ring depends on the principal moments of inertia of its cross section (I_{xx}, I_{yy}) as well as its mean radius a_r. A stiffening end-ring is efficient if the boundary to which it is attached, can reach, within a certain difference, the totally fixed condition with a minimum weight ratio W_r (weight of ring/weight of shell). These factors affecting stiffness and efficiency, therefore suggest the definition of stiffness factors of the form

$$S_{tx} = \frac{r_x}{r}(W_r \widetilde{a})^{1/2}, \qquad S_{ty} = \frac{r_y}{r}(W_r \widetilde{a})^{1/2}$$

where

$$r_x = \frac{1}{a_r}\left(\frac{I_{xx}}{A_r}\right)^{1/2}, \qquad r_y = \frac{1}{a_r}\left(\frac{I_{yy}}{A_r}\right)^{1/2},$$

$$r = \frac{h}{(12)^{1/2}a}, \qquad \widetilde{a} = \frac{a_r}{a}$$

A_r is the cross sectional area of the ring. The out-of-plane stiffness factor S_{tx} will be taken to represent the stiffness of the ring since it controls the axial boundary conditions of the shell.

The coordinate system, displacements, rotation and resultant forces and moments are shown in Fig. 4. The uncoupled differential equations in terms of displacements for the shell are given by Eqs. (1–4) in Appendix B. The governing differential equations for the ring, derived by

6

Love (on pp. 397 and 451 of Ref. 10) will be used in this analysis. These equations include the following quantities:

(1) In-plane displacements in curvature.

(2) Transverse shear in the in-plane equilibrium equations.

(3) In-plane inertia.

(4) Rotary inertia.

It is shown in Ref. 8 that the first three quantities have a large effect on the eigenfrequencies of the ring at low circumferential wave number n and that their effect is independent of the radii of gyration r_x and r_y. However the error by neglecting rotary inertia was shown to be of $o(r^2 n^2/2)$ and since, in our case, r_x and r_y can reach $o(10^{-1})$, rotary inertia must be included for $n \geq 3$.

The in-plane and out-of-plane motions of the ring can be uncoupled due to the symmetry of the cross section leading to the following two systems of differential equations:

$$[D_{r,ij}^{(i)}] \begin{Bmatrix} v_r \\ w_r \end{Bmatrix} = \{F_{r,i}^{(i)}\},$$
$$\qquad\qquad i,j = 1,2 \qquad (12)$$
$$[D_{r,ij}^{(o)}] \begin{Bmatrix} u_r \\ \beta_r \end{Bmatrix} = \{F_{r,i}^{(o)}\},$$

$\{F_{r,i}^{(i)}\}$ and $\{F_{r,i}^{(o)}\}$ are forcing functions that depend on the nondimensional stress resultants of the shell at the boundary where the ring is connected. The differential operators and forcing functions in Eq. (12) are given in Appendix D.

For free vibration, the exact solution and resulting ordinary differential equations for the shell, are given in Appendix B. For the ring, Eq. (12) has an exact solution of the form:

$$v_r = v_{rn} \cos(n\theta) \sin(\widetilde{\omega}\tau)$$

$$\begin{Bmatrix} w_r \\ u_r \\ \beta_r \end{Bmatrix} = \begin{Bmatrix} w_{rn} \\ u_{rn} \\ \beta_{rn} \end{Bmatrix} \sin(n\theta) \sin(\widetilde{\omega}\tau)$$

$$\{F_{r,i}^{(i)}\} = \{F_{r,ni}^{(i)}\} \sin(n\theta) \sin(\widetilde{\omega}\tau)$$

$$\{F_{r,i}^{(o)}\} = \{F_{r,ni}^{(o)}\} \sin(n\theta) \sin(\widetilde{\omega}\tau)$$

$$(13)$$

Upon substitution of Eq. (13) in Eq. (12) we obtain the following system of linear algebraic equations:

$$[L_{r,ij}^{(i)}] \begin{Bmatrix} v_{rn} \\ w_{rn} \end{Bmatrix} = \{F_{r,ni}^{(i)}\},$$
$$\qquad\qquad i,j = 1,2 \qquad (14)$$
$$[L_{r,ij}^{(o)}] \begin{Bmatrix} u_{rn} \\ \beta_{rn} \end{Bmatrix} = \{F_{r,ni}^{(o)}\},$$

The constant matrices in Eq. (14) are given in Appendix D. Solving for v_{rn}, w_{rn}, u_{rn} and β_{rn} in Eq. (14) and rearranging terms

$$\begin{Bmatrix} w_{rn} \\ u_{rn} \\ v_{rn} \\ \beta_{rn} \end{Bmatrix} = [M_{d,ij}] \begin{Bmatrix} \widetilde{q}_{xx}(\ell/2) \\ \widetilde{n}_{xx}(\ell/2) \\ \widetilde{n}_{x\theta}(\ell/2) \\ \widetilde{m}_{xx}(\ell/2) \end{Bmatrix}, \qquad i,j = 1 \text{ to } 4 \qquad (15)$$

The right hand vector is composed of the nondimensional stress and moment resultants of the shell evaluated at the boundary where the ring is connected. Appendix D gives $[M_{d,ij}]$. The final step in the analysis is the matching of the displacements and slope at the boundary of the shell with the displacements and rotation of the ring. This is given by the following relationship:

$$\begin{Bmatrix} w_{rn} \\ u_{rn} \\ v_{rn} \\ \beta_{rn} \end{Bmatrix} = [M_{T,ij}] \begin{Bmatrix} w_n(\ell/2) \\ u_n(\ell/2) \\ v_n(\ell/2) \\ w_n'(\ell/2) \end{Bmatrix}, \qquad i,j = 1 \text{ to } 4 \qquad (16)$$

Appendix D gives $[M_{T,ij}]$. Eliminating the ring displacement vector from the left hand sides of Eqs. (15) and (16) we obtain four homogeneous boundary conditions relating the displacements and slope of the shell at the ring boundary to the nondimensional normal stress and moment resultants of the shell at the same boundary:

$$[M_{T,ij}] \begin{Bmatrix} w_n(\ell/2) \\ u_n(\ell/2) \\ v_n(\ell/2) \\ w_n'(\ell/2) \end{Bmatrix} = [M_{d,ij}] \begin{Bmatrix} q_{xx}(\ell/2) \\ n_{xx}(\ell/2) \\ n_{x\theta}(\ell/2) \\ m_{xx}(\ell/2) \end{Bmatrix} \qquad (17)$$

The procedure for the determination of the exact eigenfrequencies is then similar to the one adopted in Section II C earlier in this report.

The eigenfrequencies for a shell with $a/h = 400$ were calculated for two different length ratios, $\ell = 1$ and 2, and for a ring stiffness factor S_{tx} in the range

$$5 \leq S_{tx} \leq 260$$

(a) RING WITH H-TYPE SECTION

$h_e = (H + h_r + h)/2$

$D/H = 1.4$

$H/h_r = 6.0$
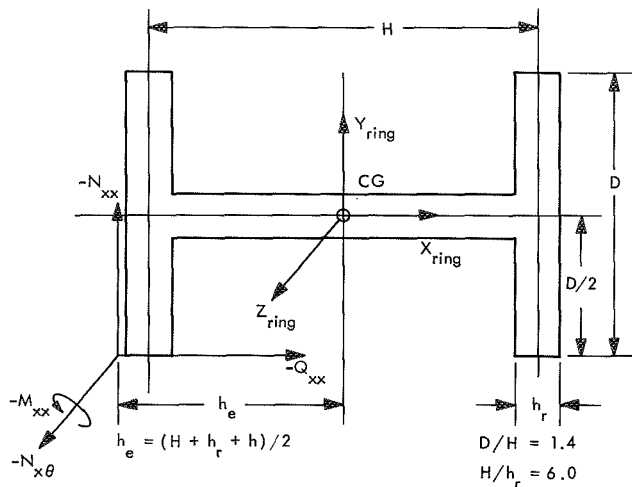
(b) RING WITH THIN RECTANGULAR CLOSED SECTION

$h_e = (H + h_r + h)/2$

$D/H = 1.3$

$H/h_r = 5.0$
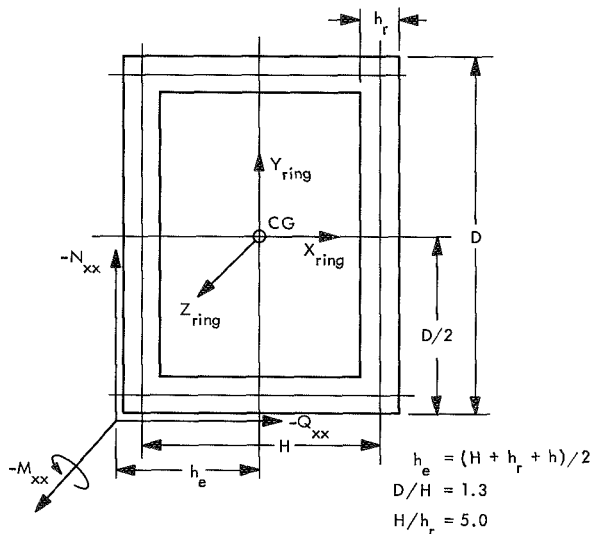
(c) RING WITH RECTANGULAR SOLID SECTION

$h_e = (H + h_r + h)/2$

$D/H = 2.0$

$H/h_r = 1.0$
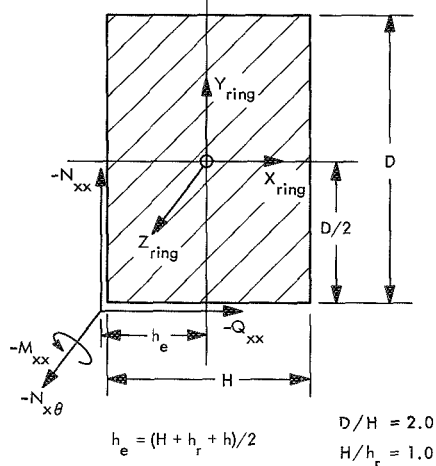
Fig. 5. Sign convention and dimension notation for ring with different sections

which corresponds to a weight ratio W_r in the range: $0.2 \leq Wr \leq 7.5$. The dimensions of the ring cross sections are shown in Fig. 5a, b, and c. The above computations were performed for boundary condition

FXR/FXR: (fixed with flexible ring at both ends)

For each eigenfrequency, the $\% d_f$

$$\% d_f = \left(\frac{\widetilde{\omega}_{fxr}}{\widetilde{\omega}_{fx2}} - 1 \right) 100$$

was plotted against S_{tx} and W_r for boundary condition *FXR/FXR* for modes with $n \geq 5$ and with one half axial wave $(m = 1)$, since at this value of m, the $\% d_f$ is largest. For low circumferential wave number with $n = 2$, $n = 3$, and $n = 4$, the $\widetilde{\omega}_{LF}$ corresponding to the first three modes was plotted against S_{tx} and W_r as shown in Figs. 6–8 for the H-type section only. Similar curves apply to all the other sections.
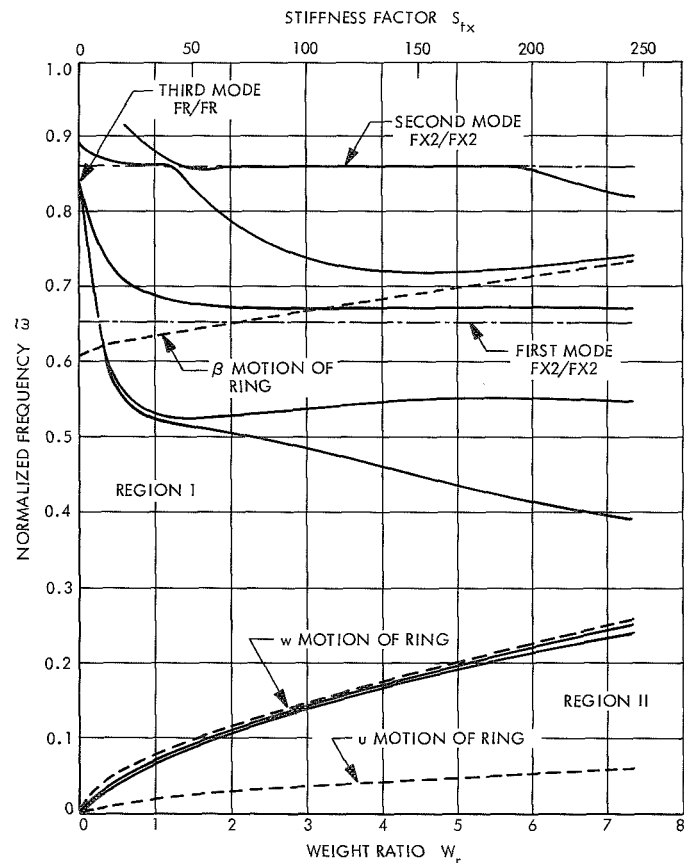
Fig. 6. Asymptotic behavior of $\widetilde{\omega}$ with S_{tx} and W_r for the first three modes with $n = 2$, $l = 1$, $a/h = 400$
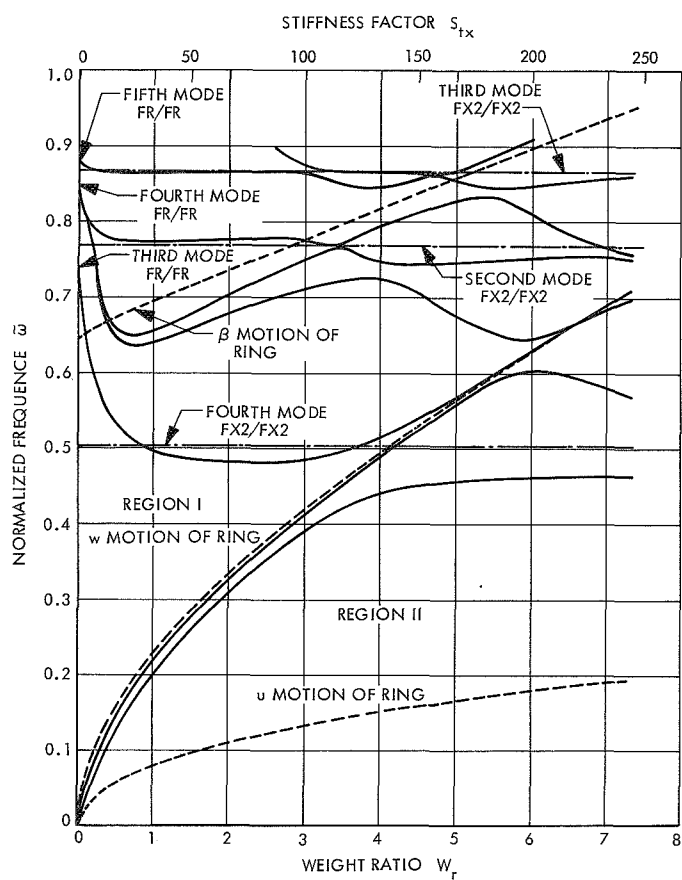
Fig. 7. Asymptotic behavior of $\tilde{\omega}$ with S_{tx} and W_r for the first three modes with $n = 3$, $\ell = 1$, $a/h = 400$
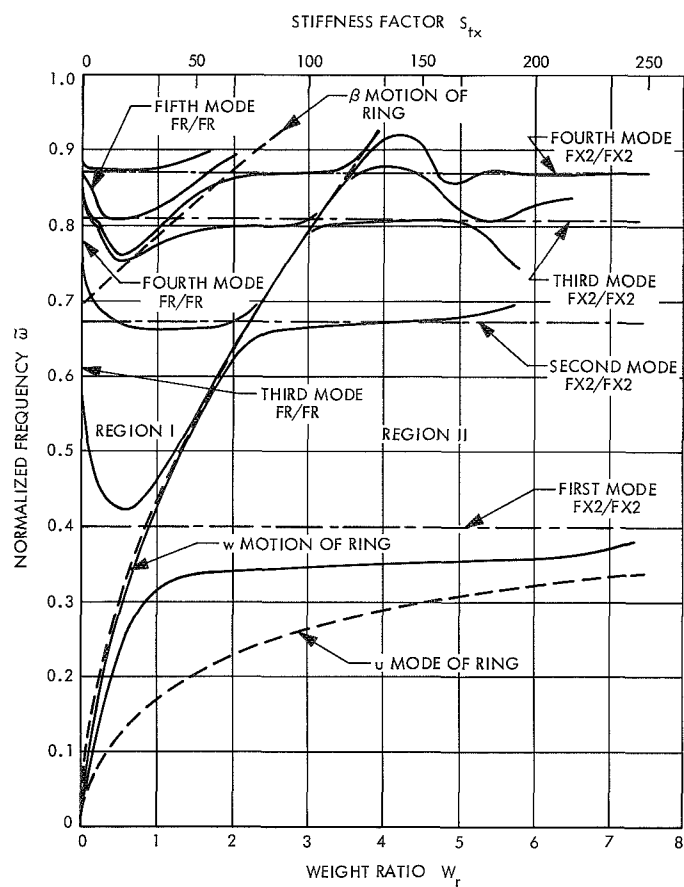
Fig. 8. Asymptotic behavior of $\tilde{\omega}$ with S_{tx} with W_r for the first three modes with $n = 4$, $\ell = 1$, $a/h = 400$

IV. Theoretical Conclusions

The influence of an elastic ring on the eigenfrequencies of the ring-shell system is different for various values of the circumferential wave number n. This results since the ring frequencies are monotonously increasing with n whereas the shell low frequencies exhibit a minimum. We distinguish three different ranges of circumferential wave number n:

(1) For small values of n ($n = 2$), both the w and u predominant ring frequencies are lower than the free/free shell frequencies for the range of stiffness parameters S_{tx} of interest and there is no mode interaction except for very large values of S_{tx}.

(2) For intermediate n ($n = 3, 4$), the w and u ring frequencies are nearly of the same magnitude as the free/free shell frequencies for the range of S_{tx} of interest and considerable mode interaction is evidenced.

(3) For large values of n ($n \geqq 5$), the ring frequencies are considerably higher than the shell frequencies even for small but finite ring stiffness parameter S_{tx}. The region of interaction is confined to very small values of S_{tx} below the range of interest.

The most interesting range is the one with intermediate n and will now be discussed in more detail. The variation of $\tilde{\omega}_{LF}$ with S_{tx} and W_r is shown in Fig. 7 for the first three modes with $n = 3$ for the H-type section. The ring itself has four eigenfrequencies:

(1) w predominant in-plane eigenfrequency
$$\tilde{\omega}_{r,1} = 0\,(r_y\,n^2) \to 0 \text{ as } S_{tx} \to 0$$

(2) v predominant in-plane eigenfrequency
$$\tilde{\omega}_{r,2} = 0\,(n^2 + 1)^{\frac{1}{2}} \text{ (independent of } S_{tx})$$

(3) u predominant out-of-plane eigenfrequency
$$\tilde{\omega}_{r,3} = 0\,(r_x\,n^2) \to 0 \text{ as } S_{tx} \to 0$$

(4) β predominant out-of-plane eigenfrequency

$$\tilde{\omega}_{r,4} = 0\left[\frac{r_t}{r_p}\left(\frac{n^2}{2\,(1+\nu)} + \frac{r_x^2}{r_t^2}\right)^{\frac{1}{2}}\right]$$

$$\to \text{ finite value as } S_{tx} \to 0$$

where (S_{tx}/S_{ty}) is held constant. The asymptotic behavior of the first five eigenfrequencies of the shell-ring system is now described in detail. Let Regions I and II in Fig. 7 be the regions in the left and right sides of the $\tilde{\omega}_{r,1}$ line respectively.

A. The First and Second System Eigenfrequencies

The first two system eigenfrequencies $\tilde{\omega}_{s,1}$ and $\tilde{\omega}_{s,2}$ approach the first two frequencies corresponding to boundary condition FR/FR (free/free) as S_{tx} goes to zero in Region I. These are ring predominant frequencies that become asymptotic to $\tilde{\omega}_{r,1}$ for some range of S_{tx} then change asymptote to the first frequency of $FX2/FX2$ (totally fixed at both edges) in Region II.

B. The Third System Eigenfrequency

The third system eigenfrequency $\tilde{\omega}_{s,3}$ approaches the third frequency of FR/FR at S_{tx} goes to zero in Region I, then becomes asymptotic to $\tilde{\omega}_{r,1}$ in the neighborhood where $\tilde{\omega}_{s,1}$ changes asymptote. After some range of S_{tx}, $\tilde{\omega}_{s,3}$ changes asymptote to the first frequency of $FX2/FX2$ in Region II.

C. The Fourth and Fifth System Eigenfrequencies

The last two system eigenfrequencies $\tilde{\omega}_{s,4}$ and $\tilde{\omega}_{s,5}$ approach the fourth frequency of FR/FR as S_{tx} goes to zero in Region I. They then follow the β ring frequency and in the neighborhood where $\tilde{\omega}_{s,3}$ changes asymptote, the $\tilde{\omega}_{s,4}$ shifts asymptote to $\tilde{\omega}_{r,1}$. A second change of asymptote occurs at some S_{tx} to the second frequency of $FX2/FX2$ in Region II.

The change of asymptotes for each of the above three modes can be explained in the following way. Since the system is linear elastic, governed by formally self-adjoint differential equations having unmixed natural boundary conditions, each system eigenvalue must have only one independent eigenfunction.[3] This implies that crossing of the three lines representing the first three system eigenfrequencies is impossible.

At first one might expect that eight (symmetric boundary conditions) additional system frequencies will be induced due to the introduction of the four ring eigenfrequencies in the free/free shell spectrum. However, only four additional system modes are excited. The first two modes are $\tilde{\omega}_{s,4}$ and $\tilde{\omega}_{s,5}$ and are induced by the β predominant ring frequency $\tilde{\omega}_{r,4}$, and the other two are v predominant system frequencies induced by the v predominant ring frequency $\tilde{\omega}_{r,2}$. The following argument shows that no system frequency can be induced by either the w or the u predominant ring frequencies $\tilde{\omega}_{r,1}$ and $\tilde{\omega}_{r,3}$. Assume at first that one of these ring frequencies induces a system frequency $\tilde{\omega}_{s,4}$. This system frequency cannot

---

[3]See Appendix E.

follow $\tilde{\omega}_{r,1}$ nor $\tilde{\omega}_{r,3}$ to zero as S_{tx} goes to zero since as this limit is approached, the system frequency must converge to a free/free shell eigenfrequency in a continuous manner. The only possible ring frequency that can induce $\tilde{\omega}_{s,4}$ is then $\tilde{\omega}_{r,4}$ the β predominant frequency, which has a finite value at $S_{tx} = 0$. The w motion in $\tilde{\omega}_{s,4}$ is induced by the torsion and eccentricity of the ring cross section. Following the same argument, we expect that the v predominant ring frequency $\tilde{\omega}_{r,2}$ induces an additional system frequency which approaches the $\tilde{\omega}_{HF}$ corresponding to the first high frequency mode for boundary condition (free/free).

One can see from Fig. 7 that the third system frequency $\tilde{\omega}_{s,3}$ is higher than the $FX2/FX2$ frequency for low values of S_{tx}. This can be explained as follows. The $\tilde{\omega}_{s,3}$ is out-of-phase with $\tilde{\omega}_{r,1}$ in that range of S_{tx}. The ring being very weak, will exhibit relatively large amplitudes and due to the change in phase, the corresponding mode shape will have one circumferential node near each ring boundary. The axial wave number m will be greater than one. And since $\tilde{\omega}_{LF}$ is monotonously increasing with m, it follows that $\tilde{\omega}_{s,3}$ will be higher than $\tilde{\omega}_{FX2}$, noting that the axial restraint has little effect on the frequency at $n = 3$. As S_{tx} increases, the ring becomes stiffer and consequently its amplitude becomes smaller, thus shifting the circumferential node towards the boundary. This shift tends to decrease m hence a decrease in $\tilde{\omega}_{s,3}$.

The same conclusions apply for $n = 2$ with the only difference that the change in asymptotes occurs outside the S_{tx} range of interest (See Fig. 6). As n becomes higher $(n \geqq 4)$, the $\tilde{\omega}_{r,1}$ line becomes steeper, thus confining region I to very small values of S_{tx} (See Fig. 8).

For large values of circumferential wave number n $(n \geqq 5)$, the FXR/FXR (free with elastic ring at both ends) eigenfrequencies are smaller than the corresponding ones for $FX2/FX2$ (totally fixed at both edges), as shown in Figs. 9–12. The rate of overall shell stiffness increase, which is measured by the magnitude of the eigenfrequency for some mode shape, depends on the type of section.

For an H open-type section (Figs. 9 and 10) the $\%d_f$ decreases slowly and monotonously with the stiffness factor S_{tx}. The $\%d_f$ defined by

$$\%d_f = 100\left(\frac{\tilde{\omega}_{FXR}}{\tilde{\omega}_{FX2}} - 1\right)$$

increases with n for fixed values of S_{tx} until it reaches a maximum at some $n = n^*$, after which the $\%d_f$ decreases with n. This can be explained as follows. It is seen from Fig. 2b that the

$$(\%d)_{FX2} = 100\left(\frac{\tilde{\omega}_{FX2}}{\tilde{\omega}_{SS1}} - 1\right)$$

exhibits a maximum at some value of n which is smaller than n at which $\tilde{\omega} = (\tilde{\omega})_{min}$. This shows that at this value
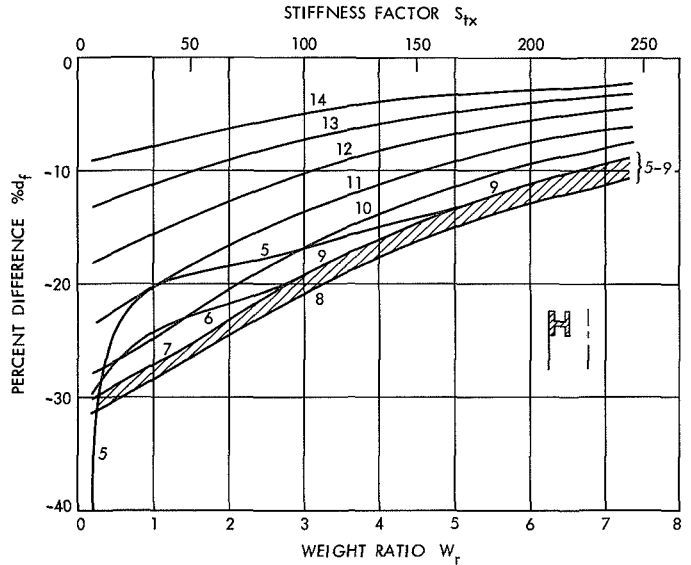

Fig. 9. Variation of $\%d_f$ with S_{tx} and W_r for a shell with H-type end rings; $l = 1$, $a/h = 400$, $m = 1$, $n \geqq 5$
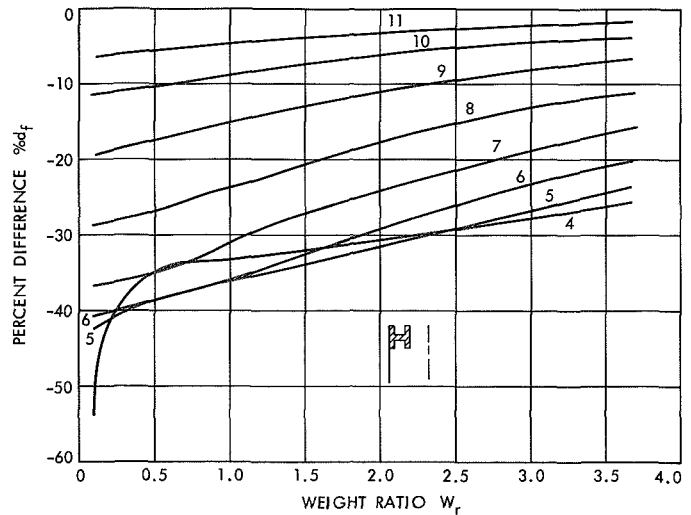

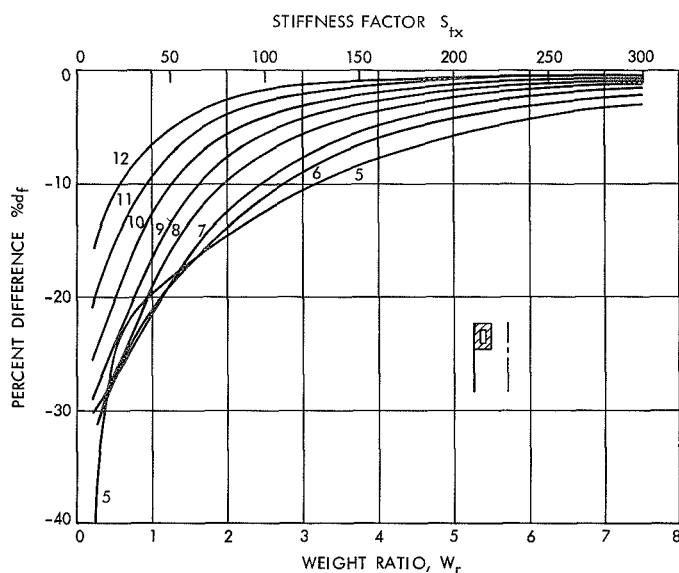Fig. 10. Variation of $\%d_f$ with W_r for a shell with H-type end rings; $l = 2$, $a/h = 400$, $m = 1$, $n \geqq 4$

STIFFNESS FACTOR S_{tx}

PERCENT DIFFERENCE $\%d_f$

WEIGHT RATIO, W_r

Fig. 11. Variation of $\% d_f$ with S_{tx} and W_r for a shell with hollow thin rectangular closed end rings; $l = 1$, $a/h = 400$, $m = 1$, $n \geq 5$
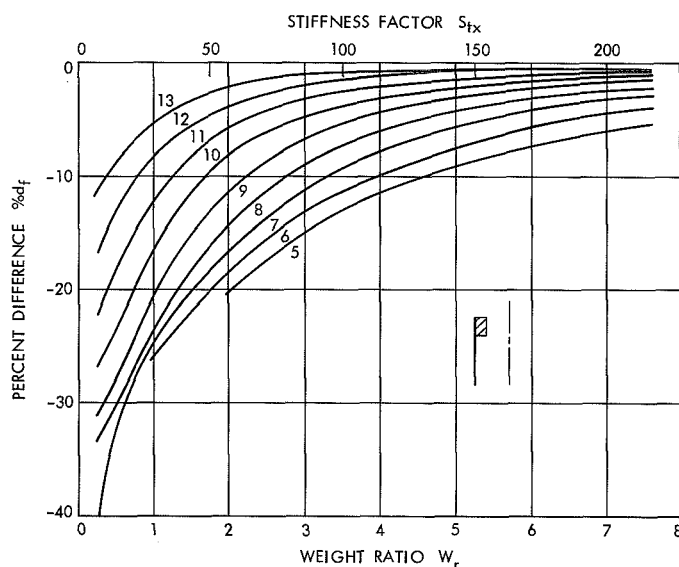

STIFFNESS FACTOR S_{tx}

PERCENT DIFFERENCE $\%d_f$

WEIGHT RATIO W_r

Fig. 12. Variation of $\% d_f$ with S_{tx} and W_r for a shell with solid rectangular end rings; $l = 1$, $a/h = 400$, $m = 1$, $n \geq 5$

of n, the axial restraint in the boundaries is the most effective. The $\%d_f$ variation with S_{tx} is expected to behave in a similar fashion. For a thin rectangular closed section (Fig. 11) the rate of decrease of $\%d_f$ with S_{tx} and W_r is much faster than the corresponding rate for the open H-type section at low S_{tx} until a certain S_{tx} is reached

after which very small gain in stiffness is realized on the expanse of large increase in weight. This type of closed section thus exhibits an optimum W_r which can now be defined as the W_r at which $d\,(d_f)/dW_r$ is less than a certain allowable small number. For our specific example (Fig. 11), the optimum occurs nearly at $W_r \simeq 2.5$ for $n = 8$. The optimum W_r then decreases slowly with the circumferential wave number n. For a closed solid rectangular section (Fig. 12), the optimum stiffness exists but occurs at $W_r \simeq 3$. Calculations were performed to find the effect of ring location with respect to the shell mid-surface, by comparing the eigenfrequencies of a solid rectangular section fixed outside, inside or in the mid-surface of the shell. No appreciable difference was noticed between the three cases.

The $\%d_f$ increases with the wave length parameter l/m as can be seen by comparing Figs. 9 and 10. Consequently, a stiffer ring is required to reach a certain $\%d_f$ from $FX2/FX2$ the larger the axial wave length and the nearer the circumferential wave number n is to n^*, at which the $\%d$ of the corresponding $FX2/FX2$ shell is maximum.

It follows then that the out-of-plane stiffness of the ring as well as its torsional rigidity are responsible for the stiffening of the shell. All open sections are weak in torsion; a closed section is preferable if it does not present practical difficulties.

V. Experimental Determination of the Frequencies

A. Introduction

An experiment was carried out to check the validity of the previous theoretical analysis and demonstrate the effect of elastic rings on the eigenfrequencies of a cylindrical shell.

In Section IV of this report, it was shown that the mode shapes with predominantly membrane energy (i.e., low circumferential wave number modes) are greatly influenced by the ring stiffness. The eigenfrequencies associated with these modes differ greatly from those for the totally fixed shell, even for rings that are considered stiff in practical applications. It was also noticed that at those low circumferential wave numbers, two additional low-frequency modes were induced due to the interaction of the ring frequencies with the free shell frequencies.

The experiment consists of finding the eigenfrequencies and corresponding mode shapes of a cylindrical shell with integral end rings of rectangular cross section, located on

the outside of the shell. The details of the experiment are given in the next subsection.

B. Experimental Setup

The shell used in the experiment was machined from a seamless tube of Al 6061-T6 material. The tube was first turned on the inside and then placed on a steel mandral by heating the aluminum tube. The outside machining process was carried out on the mandral and the final shell removed by heating. The end rings were an integral part of the shell. The final nominal dimensions are shown in Fig. 13. The wall thickness variation from the nominal was ± 0.0009 in. corresponding to ± 6% variation.

The support conditions desired for the test were a free support for the shell-ring system. However, it was necessary to constrain the rigid body motion of the shell in order that the mode shapes could be readily measured. This was accomplished by mounting one end of the shell on the base plate but making only a flexible line contact with the end ring. For this purpose, the end plate was fitted with two O rings, one to support the axial motion and the other to support the radial motion. The O ring for the radial support was mounted so as to allow a few thousands of an

inch clearance. It was felt that this provided sufficient play so as not to restrict the radial motion and in the same time provide a reasonably good support.

The shell was oscillated using an acoustical driver, powered by a 75-W amplifier and variable frequency oscillator. The driver was fitted with a conical nose which had a ¼-in. circular opening. The outlet of the driver was positioned approximately 0.1 in. from the shell surface normal to it. This type of excitation forces only in the radial direction and therefore it is difficult to excite modes which are not predominantly radial motion. This will be seen in the results of the next subsection.

The response of the shell was measured using a reluctance type pickup which can traverse in the axial and circumferential directions. This equipment is described in Ref. 12. The signal from the pickup was displayed on an oscilloscope along with the input signal to the driver. It was necessary to run the pickup signal through a narrow band pass filter to remove the noise caused by the electric motors of the scanning system. This was necessary only for modes with very low amplitude (high frequencies), which in some cases was as small as 10 μ in. The mode shapes were determined by plotting the root mean square of the displacement against the circumferential distance on an x-y plotter. A count of the nodes gave the circumferential wave number n. The axial wave number was determined by just observing the signal on the oscilloscope during an axial traverse.

C. Conclusions

The theoretical frequencies $(\tilde{\omega}_{th})_{FXR}$ and the experimental frequencies $(\tilde{\omega}_{exp})_{FXR}$ for the boundary condition in the test (FXR/FXR), as well as the theoretical frequencies for the fully fixed shell $(\tilde{\omega}_{th})_{FX2}$ with the same geometrical parameters are listed in Table 3, for the following range of circumferential and axial wave numbers:

$$2 \leqq n \leqq 18, \qquad 1 \leqq m \leqq 4$$

The above three frequency spectrums are plotted in Fig. 14.

For low circumferential wave number (i.e., $\hat{n} < n$ at which $\tilde{\omega} = \tilde{\omega}_{min}$), the $(\tilde{\omega}_{exp})_{FXR}$ are lower than the $(\tilde{\omega}_{th})_{FXR}$. The percent difference $\%\tilde{d}$ defined as

ALL FIGURE DIMENSIONS IN INCHES

0.2795

0.6

8.018

7

0.01407

0.6

GEOMETRICAL PROPERTIES

RING

$\tilde{d}$ = 2.167

$\tilde{H}$ = $\tilde{h}$ = 19.865

SHELL

a/h = 284.93

ℓ = 1.75

MATERIAL PROPERTIES (AL 6061-T6)

ρ = 0.0976 lb/in.^{3}

E = 10^7 lb/in.^{2}

ν = 0.31
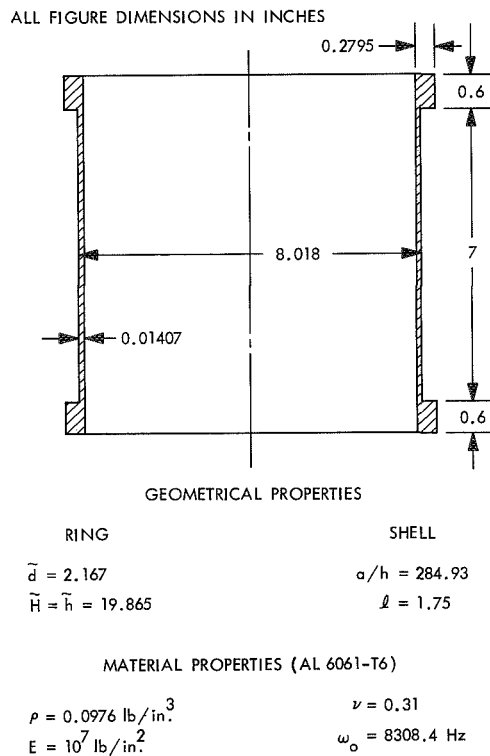
ω_o = 8308.4 Hz

Fig. 13. Properties of shell and integral rings used in the experiment

$$\%\tilde{d} = 100 \left(\frac{(\tilde{\omega}_{th})_{FXR}}{(\tilde{\omega}_{exp})_{FXR}} - 1 \right)$$

Table 3. Comparison of theoretical and experimental eigenfrequencies for boundary condition FXR/FXR; $\ell = 1.75$, $a/h = 284.93$, $\omega_0 = 8308.4$ Hz

n	m = 1			m = 2			m = 3			m = 4		
	FXR/FXR		FX2/FX2	FXR/FXR		FX2/FX2	FXR/FXR		FX2/FX2	FXR/FXR		FX2/FX2
	Experiment	Theory	Theory	Experiment	Theory	Theory	Experiment	Theory	Theory	Experiment	Theory	Theory
2		3080	3522		5992	5862		6931	6899		7349	7335
3		2240	2475		4369	4566		6146	5974		6773	6726
4	1213	1286	1826		3664	3582		5091	5067		6033	6035
5	1094	1150	1405		2504	2871		4580	4282		5472	5352
6	967	1004	1131	2123	2194	2358	3330	3444	3641		4454	4729
7	887	904	969	1854	1897	1990	2972	3037	3136	4008	4098	4190
8	861	868	900	1656	1680	1735	2647	2687	2747	3630	3682	3741
9	906	897	912	1540	1545	1578	2402	2423	2461	3314	3344	3382
10	1003	983	991	1485	1488	1507	2241	2242	2267	3070	3082	3109
11	1145	1114	1118	1524	1503	1515	2160	2141	2157	2909	2898	2916
12	1321	1280	1282	1615	1581	1588		2115	2125	2810	2789	2801
13		1473	1474	1763	1711	1716	2201	2156	2163		2751	2759
14	1747	1690	1691	1942	1884	1886	2313	2256	2261		2779	2785
16	2265	2183	2184	2409	2326	2327	2696	2600	2602	3062	3006	3009
18	2860	2739	2739	2982	2868	2868	3196	3097	3088	3490	3416	3417
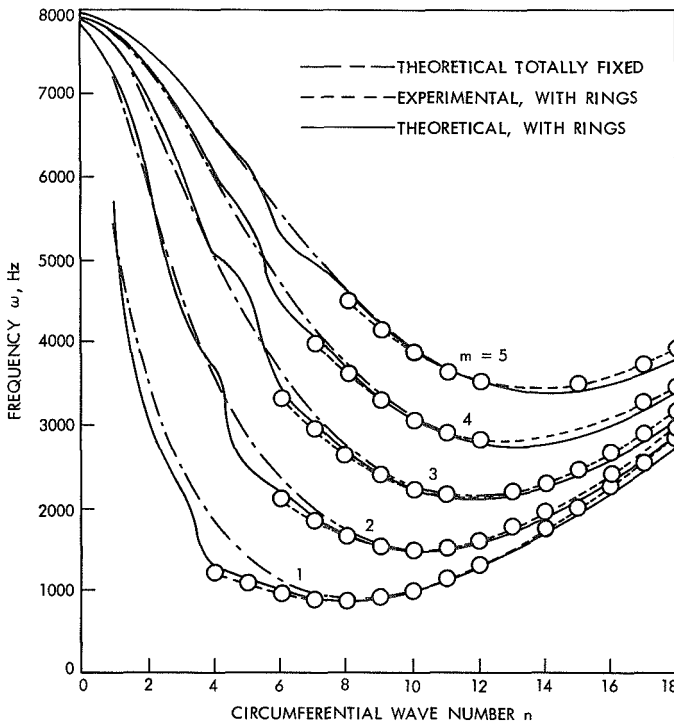
Fig. 14. Frequency spectrum for boundary condition: fixed with flexible ring at both ends; $\ell = 1.75$, $a/h = 284.93$, $\omega_0 = 8308.4$ Hz

reaches $+ 6\%$ at $n = 4$ and $m = 1$. A possible explanation for the positiveness of the $\%d$ could be the fact that the idealized ring cross section used in the analysis is assumed to keep the same shape after deformation of the ring. However, the actual section will distort under stress thus inducing more out-of-plane displacement which softens the in-plane boundary conditions of the shell and hence a decrease in frequency.

In the neighborhood of the minimum frequency $(n \simeq \hat{n})$, both $(\bar{\omega}_{exp})_{FXR}$ and $(\bar{\omega}_{th})_{FXR}$ differ by less than 0.5%. For $\hat{n} > n$, the $(\bar{\omega}_{exp})_{FXR}$ become higher than $(\bar{\omega}_{th})_{FXR}$ where we notice that the $\%d \simeq -3\%$ for all $n \geq 11$. Such a constant $\%d$ suggests the following explanation for this discrepancy. The frequency $\bar{\omega}$ can be approximated by the following relation

$$\bar{\omega}^2 = \frac{(1 - v^2)\, s^4}{(s^2 + n^2)^2} + r^2 (s^2 + n^2)^2$$

where $s = m\pi/\ell$, m is the number of axial half waves and n is the number of circumferential full waves. The above estimate is good only for qualitative analysis for boundary conditions other than SS1/SS1. The first term in this relation is the membrane contribution to the frequency and is predominant at low n $(n < \hat{n})$. The second term accounts for the bending effect and becomes predominant

at large n $(n > \hat{n})$. Both terms have the same order of magnitude in the neighborhood of the minimum frequency $(n \simeq \hat{n})$. Thus for large n, $\tilde{\omega} \simeq r \ (s^2 + n^2)$. The possibility for a constant error in ω for all $n > \hat{n}$ can exist from an error in $r = h/(12)^{\frac{1}{2}}_a$. The above argument implies that the negative $\%\tilde{d}$ for $n > \hat{n}$ is caused by an underestimation of the shell thickness. The distribution of this thickness was measured by a micrometer during manufacture and by volume considerations after manufacture. Both methods involve unavoidable errors that lead to an average thickness which was relatively inaccurate.

The $(\tilde{\omega}_{exp})_{FXR}$ differ largely from $(\tilde{\omega}_{th})_{FX2}$ at low n $(3 \leqq n \leqq 6 < \hat{n})$ as predicted by theory, in spite of the fact that the rings were sufficiently stiff.[4] This is explained by

---

[4]Weight of a ring/weight of shell $= W_r = 1.77$.

the fact that at low n, the in-plane motion which governs the in-plane boundary conditions of the shell, is comparable to the radial motion. This boundary effect dies out at large values of n $(n > \hat{n})$.

Difficulties were encountered in determining the frequencies for $\hat{n} \leqq 3$. This was probably caused by the method of excitation. Since the speaker was normal to the shell surface, mainly radial displacements were induced. Therefore, the forcing method was unable to generate in-plane displacements of sufficient magnitude, relevant with these membrane predominant modes. Much distortion was noticed in the mode shape scans at these low circumferential wave numbers due to the effect of initial imperfection and nonuniform thickness distribution.

Appendix A

Differential Operator Matrix for Cylindrical Shell Equations

$$[D_{ij}] \begin{Bmatrix} u \\ v \\ w \end{Bmatrix} = 0, \qquad i,j = 1,2,3$$

$$D_{11} = \frac{\partial^2}{\partial x^2} + \frac{1-\nu}{2} \frac{\partial^2}{\partial \theta^2} - \frac{\partial^2}{\partial \tau^2}$$

$$D_{12} = \frac{1-\nu}{2} \frac{\partial^2}{\partial x \, \partial \theta} = D_{21}$$

$$D_{13} = -\nu \frac{\partial}{\partial x} = D_{31}$$

$$D_{22} = \frac{1-\nu}{2} \frac{\partial^2}{\partial x^2} + \frac{\partial^2}{\partial \theta^2} - \frac{\partial^2}{\partial \tau^2}$$

$$D_{23} = -\frac{\partial}{\partial \theta} = D_{32}$$

$$D_{33} = 1 + r^2 \nabla^4 + \frac{\partial^2}{\partial \tau^2}$$

$$\nabla^4 = \frac{\partial^4}{\partial x^4} + 2\frac{\partial^4}{\partial x^2 \partial \theta^2} + \frac{\partial^4}{\partial \theta^4}$$

$$\nabla^2 = \frac{\partial^2}{\partial x^2} + \frac{\partial^2}{\partial \theta^2}$$

Appendix B

Uncoupling of the In-plane Displacements Equations in u and v

The uncoupled system can be written as follows:

$$\mathscr{L}(u) = \mathscr{G}_1(w) \qquad \text{(B-1)}$$

$$\mathscr{L}(v) = \mathscr{G}_2(w) \qquad \text{(B-2)}$$

$$\mathscr{R}(w) = \frac{\partial^2}{\partial \tau^2} \mathscr{H}(w) \qquad \text{(B-3)}$$

where

$$\mathscr{L} = \left(\nabla^2 - \frac{\partial^2}{\partial \tau^2} \right) \left(\nabla^2 - \frac{2}{1-\nu} \frac{\partial^2}{\partial \tau^2} \right)$$

$$\mathscr{G}_1 = \frac{\partial}{\partial x} \left\{ \nu \frac{\partial^2}{\partial \theta^2} - \frac{\partial^2}{\partial \theta^2} - \frac{2\nu}{1-\nu} \frac{\partial^2}{\partial \tau^2} \right\}$$

$$\mathscr{G}_2 = \frac{\partial}{\partial \theta} \left\{ (2+\nu) \frac{\partial^2}{\partial x^2} + \frac{\partial^2}{\partial \theta^2} - \frac{2}{1-\nu} \frac{\partial^2}{\partial \tau^2} \right\}$$

$$\mathscr{R} = r^2 \nabla^8 + \frac{\partial^2}{\partial \tau^2} \nabla^4 + (1-\nu^2) \frac{\partial^4}{\partial x^4}$$

$$\mathscr{H} = \left(\frac{3-\nu}{1-\nu} \nabla^2 - \frac{2}{1-\nu} \frac{\partial^2}{\partial \tau^2} \right) \left(r^2 \nabla^4 + \frac{\partial^2}{\partial \tau^2} \right)$$
$$+ \nabla^2 - \frac{2}{1-\nu} \frac{\partial^2}{\partial \tau^2} + 2(1+\nu) \frac{\partial^2}{\partial x^2}$$

If tangential inertia is neglected, $\mathscr{H}(w) = 0$. The system of differential equations given by Eqs. (B-1) through (B-3) is valid for *asymmetric motion*, i.e., $\partial/\partial\theta \neq 0$. However for axisymmetric motion, i.e., $\partial/\partial\theta = 0$, $v = 0$, the governing set of equations is

$$\left(\frac{\partial^2}{\partial x^2} - \frac{\partial^2}{\partial \tau^2} \right) u = \nu \frac{\partial w}{\partial x}$$

$$\left\{ \left(\frac{\partial^2}{\partial x^2} - \frac{\partial^2}{\partial \tau^2} \right) \left(r^2 \frac{\partial^4}{\partial x^4} + 1 + \frac{\partial^2}{\partial \tau^2} \right) - \nu^2 \frac{\partial^2}{\partial x^2} \right\} w = 0 \qquad \text{(B-4)}$$

For free vibration, an exact solution to the system of Eqs. (B-1) through (B-3) can be written as follows:

$$\begin{Bmatrix} u \\ v \\ w \end{Bmatrix} = \begin{Bmatrix} u_n(x) \sin(n\theta) \\ v_n(x) \cos(n\theta) \\ w_n(x) \sin(n\theta) \end{Bmatrix} \sin(\bar{\omega}\tau) \qquad \text{(B-5a)}$$

Upon substitution of Eq. (B-5a) in Eqs. (B-1) through (B-4) we obtain the following two systems of linear ordinary differential equations:

$$\left. \begin{array}{l} \mathscr{L}_n(u_n) = \mathscr{G}_{1n}(w_n), \\ \mathscr{L}_n(v_n) = \mathscr{G}_{2n}(w_n), \\ \mathscr{R}_n(w_n) = -\bar{\omega}^2 \mathscr{H}_n(w_n), \end{array} \right\} \qquad n \geq 1 \qquad \text{(B-5b)}$$

$$\left. \begin{array}{l} \mathscr{L}_o(u_o) = \nu \dfrac{dw_o}{dx}, \\ \mathscr{R}_o(w_o) = 0, \end{array} \right\} \qquad n = 0 \qquad \text{(B-5c)}$$

where

$$\mathscr{L}_n = \left(\frac{d^2}{dx^2} - \beta_1^2 \right) \left(\frac{d^2}{dx^2} - \beta_2^2 \right)$$

$$\mathscr{G}_{1n} = \frac{d}{dx} \left[\nu \frac{d^2}{dx^2} + (1+\nu)n^2 - \nu\beta_2^2 \right]$$

$$\mathscr{G}_{2n} = n \left((2+\nu) \frac{d^2}{dx^2} - \beta_2^2 \right)$$

$$\mathscr{R}_n = r^2 \bar{\nabla}_n^8 - \bar{\omega}^2 \bar{\nabla}_n^4 + (1-\nu^2) \frac{d^4}{dx^4}$$

$$\mathscr{H}_n = \left(\frac{3-\nu}{1-\nu} \bar{\nabla}_n^2 + \frac{2\bar{\omega}^2}{1-\nu} \right) (r^2 \bar{\nabla}_n^4 - \bar{\omega}^2)$$
$$+ (3+2\nu) \frac{d^2}{dx^2} - \beta_2^2$$

$$\mathscr{L}_o = \frac{d^2}{dx^2} + \bar{\omega}^2$$

$$\mathscr{R}_o = \left(\frac{d^2}{dx^2} + \bar{\omega}^2 \right) \left(r^2 \frac{d^4}{dx^4} + 1 - \bar{\omega}^2 \right) - \nu^2 \frac{d^2}{dx^2}$$

$$\beta_1^2 = n^2 - \bar{\omega}^2; \quad \beta_2^2 = n^2 - \frac{2}{1-\nu} \bar{\omega}^2$$

$$\bar{\nabla}_n^2 = \frac{d^2}{dx^2} - n^2$$

$$\bar{\nabla}_n^4 = \bar{\nabla}_n^2(\bar{\nabla}_n^2) = \frac{d^4}{dx^4} - 2n^2 \frac{d^2}{dx^2} + n^4$$

Appendix C

Dispersion Relation for Cylindrical Shells

Characteristic equation (dispersion relation) for $n = 0$:

$$C_o(1)\,\lambda_{oj}^6 + C_o(2)\,\lambda_{oj}^4 + C_o(3)\,\lambda_{oj}^2 + C_o(4) = 0$$

$$C_o(1) = r^2$$

$$C_o(2) = r^2\tilde{\omega}^2$$

$$C_o(3) = 1 - \nu^2 - \tilde{\omega}^2$$

$$C_o(4) = \tilde{\omega}^2(1 - \tilde{\omega}^2)$$

Characteristic equation (dispersion relation) for $n \geq 1$:

$$C_n(1)\,\lambda_{nj}^8 + C_n(2)\,\lambda_{nj}^6 + C_n(3)\,\lambda_{nj}^4 + C_n(4)\,\lambda_{nj}^2 + C_n(5) = 0$$

$$C_n(1) = r^2$$

$$C_n(2) = r^2\left[\frac{3-\nu}{1-\nu}\tilde{\omega}^2 - 4n^2\right]$$

$$C_n(3) = r^2\left(6n^4 - \frac{3(3-\nu)}{(1-\nu)}\tilde{\omega}^2 n^2 + \frac{2\tilde{\omega}^4}{(1-\nu)}\right) + 1 - \nu^2 - \tilde{\omega}^2$$

$$C_n(4) = r^2 n^2\left(-4n^4 + \frac{3(3-\nu)}{(1-\nu)}\tilde{\omega}^2 n^2 - \frac{4\tilde{\omega}^4}{(1-\nu)}\right) + 2\left[2n^2 - \frac{3-\nu}{1-\nu}\tilde{\omega}^2 + 3 + 2\right]$$

$$C_n(5) = r^2 n^4\left(n^4 - \frac{3-\nu}{1-\nu}\tilde{\omega}^2 n^2 + \frac{2\tilde{\omega}^4}{1-\nu}\right) + \tilde{\omega}^2\left[n^2\left(-n^2 - 1 + \tilde{\omega}^2\frac{3-\nu}{1-\nu}\right) + \frac{2\tilde{\omega}^2}{1-\nu}(1-\tilde{\omega}^2)\right]$$

Appendix D

Differential Operators and Influence Matrices for the End-Ring

The uncoupled differential equations for the ring are

$$[D_{r,ij}^{(i)}] \begin{Bmatrix} v_r \\ w_r \end{Bmatrix} = \{F_{r,i}^{(i)}\},$$

$$i,j = 1,2 \qquad \text{(D-1)}$$

$$[D_{r,ij}^{(o)}] \begin{Bmatrix} u_r \\ \beta_r \end{Bmatrix} = \{F_{r,i}^{(o)}\},$$

where

$$D_{r,11}^{(i)} = -\frac{\partial}{\partial\theta}\left[\frac{\partial^2}{\partial\theta^2} + 1 - \frac{a^2}{(1-\nu^2)}\frac{\partial^2}{\partial\tau^2}\right]$$

$$D_{r,12}^{(i)} = \frac{\partial^2}{\partial\theta^2} + 1 + \frac{\tilde{a}^2}{(1-\nu^2)}\frac{\partial^2}{\partial\tau^2}$$

$$D_{r,21}^{(i)} = \frac{\partial}{\partial\theta}\left[r_y^2\frac{\partial^2}{\partial\theta^2} - 1 - r_y^2\frac{\tilde{a}^2}{(1-\nu^2)}\frac{\partial^2}{\partial\tau^2}\right]$$

$$D_{r,22}^{(i)} = r_y^2\frac{\partial^4}{\partial\theta^4} + 1 + \frac{\tilde{a}^2}{1-\nu^2}\frac{\partial^2}{\partial\tau^2}\left(1 - r_y^2\frac{\partial^2}{\partial\theta^2}\right)$$

$$D_{r,11}^{(o)} = r_x^2\frac{\partial^4}{\partial\theta^4} - \frac{r_t^2}{2(1+\nu)}\frac{\partial^2}{\partial\theta^2} + \frac{\tilde{a}^2}{1-\nu^2}\frac{\partial^2}{\partial\tau^2}\left(1 - r_x^2\frac{\partial^2}{\partial\theta^2}\right)$$

$$D_{r,12}^{(o)} = -\left[r_x^2 + \frac{r_t^2}{2(1+\nu)}\right]\frac{\partial^2}{\partial\theta^2} = D_{r,21}^{(o)}$$

$$D_{r,22}^{(o)} = -\left[\frac{r_t^2}{2(1+\nu)}\frac{\partial^2}{\partial\theta^2} - r_x^2 - r_p^2\frac{\tilde{a}^2}{(1-\nu^2)}\frac{\partial^2}{\partial\tau^2}\right]$$

$$\{F_{r,i}^{(i)}\} = \begin{bmatrix} f_{c1} & f_{c2} \\ f_{c1} & -f_{c3}\end{bmatrix} \begin{Bmatrix} q_{xx}(\ell/2) \\ \dfrac{\partial n_{x\theta}(\ell/2)}{\partial\theta}\end{Bmatrix}$$

$$\{F_{r,i}^{(o)}\} = \begin{bmatrix} -f_{c4} & f_{c7} & 0 & 0 \\ f_{c5} & 0 & -f_{c6} & f_{c1}\end{bmatrix}\begin{Bmatrix} n_{xx}(\ell/2) \\ \dfrac{\partial n_{x\theta}(\ell/2)}{\partial\theta} \\ q_{xx}(\ell/2) \\ m_{xx}(\ell/2)\end{Bmatrix}$$

Constant factors f_{ck} ($k=1$ to 7) depend on the cross section properties of the ring and are given in Table D-1 for an H-type section. For free vibration, system (D-1) has an exact solution as given by Eq.(13) in the body of this

Table D-1. Ring geometrical parameters and related coefficients

$$\tilde{d} = \frac{D}{H}$$
$$\tilde{h} = \frac{h_r}{h}$$
$$\tilde{a} = \frac{a_r}{a}$$
$$\tilde{H} = \frac{H}{h_r}$$

Nondimensional symbol	Equivalent relation
$\tilde{A}_r = \dfrac{A_r}{h_r^2}$	$(1 + 2\tilde{d})\tilde{H}$
$\tilde{h}_e = \dfrac{h_e}{h_r}$	$\dfrac{\tilde{H} + 1 + \frac{1}{\tilde{h}}}{2}$
$r_t = \dfrac{1}{a_r}\left(\dfrac{J_{eff}}{A_r}\right)^{1/2}$	$\dfrac{h\tilde{h}}{a_r}\left(\dfrac{1}{3} - \dfrac{0.6301875}{\tilde{H}(1+2\tilde{d})}\right)^{1/2}$
$r_x = \dfrac{1}{a_r}\left(\dfrac{I_{xx}}{A_r}\right)^{1/2}$	$\dfrac{h\tilde{h}}{a_r}\left(\dfrac{1+2\tilde{H}^2\tilde{d}^3}{12(1+2\tilde{d})}\right)^{1/2}$
$r_y = \dfrac{1}{a_r}\left(\dfrac{I_{yy}}{A_r}\right)^{1/2}$	$\dfrac{h\tilde{h}}{a_r}\left(\dfrac{\tilde{H}^2 + 2\tilde{d}(1 + 3\tilde{H}^2)}{12(1 + 2\tilde{d})}\right)^{1/2}$
$R_{hr} = \dfrac{a_r}{h}$	$\dfrac{a}{h} - \dfrac{1 + \tilde{h}(1 + \tilde{H})}{2}$
$W_r = \dfrac{\text{(weight ring)}}{\text{(weight shell)}}$	$\dfrac{a_r}{h}\dfrac{\tilde{A}_r\tilde{h}}{\left[\frac{a}{h}\right]^2}$
S_{tx}, S_{ty}	$\dfrac{r_x}{r}(W_r\tilde{a})^{1/2}, \dfrac{r_y}{r}(W_r\tilde{a})^{1/2}$
f_{c1}	$\left[12(1-\nu^2)\left(\dfrac{a}{h}\right)\tilde{A}_r\tilde{h}^2\right]^{-1}$
f_{c2}	$\dfrac{\frac{a}{h}}{2(1+\nu)\tilde{A}_r\tilde{h}^2}$
f_{c3}	$\dfrac{\tilde{h}_e}{2(1+\nu)\tilde{A}_r\tilde{h}}$
f_{c4}	$\dfrac{2}{(1-\nu)}f_{c2}$
f_{c5}	$\dfrac{2}{(1-\nu)}f_{c3}$
f_{c6}	$\dfrac{\tilde{d}\tilde{h}}{24(1-\nu^2)\left(\frac{a}{h}\right)^2\tilde{A}_r\tilde{h}}$
f_{c7}	$\dfrac{\tilde{d}\tilde{h}}{2\tilde{h}_e}f_{c3}$

report. Such a solution leads to a system of algebraic linear equations of the form:

$$[L^{(i)}_{r,ij}] \quad \left\{ \begin{matrix} v_{rn} \\ w_{rn} \end{matrix} \right\} = \{F^{(i)}_{r,ni}\},$$

$$[L^{(o)}_{r,ij}] \quad \left\{ \begin{matrix} u_{rn} \\ \beta_{rn} \end{matrix} \right\} = \{F^{(o)}_{r,ni}\}, \qquad i,j = 1,2 \qquad \text{(D-2)}$$

where

$$L^{(i)}_{r,11} = -n\left(n^2 - 1 - \tilde{\omega}^2\right)$$

$$L^{(i)}_{r,12} = -\left(n^2 - 1 + \tilde{\omega}^2\right)$$

$$L^{(i)}_{r,21} = n\left(r_y^2 n^2 + 1 - \tilde{\omega}^2 r_y^2\right)$$

$$L^{(i)}_{r,22} = r_y^2 n^4 + 1 - \tilde{\omega}^2\left(r_y^2 n^2 + 1\right)$$

$$L^{(o)}_{r,11} = n^2 \left(r_x^2 n^2 + \frac{r_t^2}{2(1+\nu)} \right) - \tilde{\omega}^2\left(1 + r_x^2 n^2\right)$$

$$L^{(o)}_{r,12} = n^2 \left(r_x^2 + \frac{r_t^2}{2(1+\nu)} \right) = L^{(o)}_{r,21}$$

$$L^{(o)}_{r,22} = r_x^2 + \frac{r_t^2 n^2}{2(1+\nu)} - r_p^2 \tilde{\omega}^2$$

$$\tilde{\omega}^2 = \tilde{\omega}^2 \frac{\tilde{a}^2}{(1-\nu^2)}, \qquad \tilde{a} = \frac{a_r}{a}$$

and r_x, r_y, r_t and r_p are the nondimensional radii of gyration of the ring cross section.

$$\{F^{(i)}_{r,ni}\} = \begin{bmatrix} f_{c1} & -nf_{c2} \\ f_{c1} & nf_{c3} \end{bmatrix} \quad \left\{ \begin{matrix} \tilde{q}_{xx}\,(\ell/2) \\ \tilde{n}_{x\theta}\,(\ell/2) \end{matrix} \right\}$$

$$\{F^{(o)}_{r,ni}\} = \begin{bmatrix} -f_{c4} & -nf_{c7} & 0 & 0 \\ f_{c5} & 0 & -f_{c6} & f_{c1} \end{bmatrix} \left\{ \begin{matrix} \tilde{n}_{xx}\,(\ell/2) \\ \tilde{n}_{x\theta}\,(\ell/2) \\ \tilde{q}_{xx}\,(\ell/2) \\ \tilde{m}_{xx}\,(\ell/2) \end{matrix} \right\}$$

$$\left\{ \begin{matrix} n_{xx}\,(\ell/2) \\ q_{xx}\,(\ell/2) \\ m_{xx}\,(\ell/2) \end{matrix} \right\} = \left\{ \begin{matrix} \tilde{n}_{xx}\,(\ell/2) \\ \tilde{q}_{xx}\,(\ell/2) \\ \tilde{m}_{xx}\,(\ell/2) \end{matrix} \right\} \sin\,(n\theta)\,\sin\,(\tilde{\omega}\tau)$$

$$n_{x\theta}\,(\ell/2) = \tilde{n}_{x\theta}\,(\ell/2)\,\cos\,(n\theta)\,\sin\,(\tilde{\omega}\tau)$$

Solving for w_{rn}, u_{rn}, v_{rn} and β_{rn} in Eq. (D-2) we obtain

$$\left\{ \begin{matrix} w_{rn} \\ u_{rn} \\ v_{rn} \\ \beta_{rn} \end{matrix} \right\} = [M_{d,ij}] \left\{ \begin{matrix} \tilde{q}_{xx}\,(\ell/2) \\ \tilde{n}_{xx}\,(\ell/2) \\ \tilde{n}_{x\theta}\,(\ell/2) \\ \tilde{m}_{xx}\,(\ell/2) \end{matrix} \right\}, \qquad i,j = 1 \text{ to } 4 \qquad \text{(D-3)}$$

with

$$[M_{d,ij}] = \begin{bmatrix} f_{c1}\dfrac{\left(L^{(i)}_{r,21} - L^{(i)}_{r,11}\right)}{D^{(1)}_{tr}} & 0 & -n\dfrac{\left(f_{c2}L^{(i)}_{r,21} + f_{c3}L^{(i)}_{r,11}\right)}{D^{(1)}_{tr}} & 0 \\[3mm] \dfrac{f_{c6}L^{(o)}_{r,12}}{D^{(2)}_{tr}} & \dfrac{-\left(f_{c4}L^{(o)}_{r,22} + f_{c5}L^{(o)}_{r,12}\right)}{D^{(2)}_{tr}} & -n\dfrac{L^{(o)}_{r,22}f_{c7}}{D^{(2)}_{tr}} & \dfrac{+f_{c1}L^{(o)}_{r,12}}{D^{(2)}_{tr}} \\[3mm] -f_{c1}\dfrac{\left(L^{(i)}_{r,12} - L^{(i)}_{r,22}\right)}{D^{(1)}_{tr}} & 0 & n\dfrac{\left(f_{c2}L^{(i)}_{r,22} + f_{c3}L^{(i)}_{r,12}\right)}{D^{(1)}_{tr}} & 0 \\[3mm] \dfrac{-f_{c6}L^{(o)}_{r,11}}{D^{(2)}_{tr}} & \dfrac{\left(f_{c4}L^{(o)}_{r,21} + f_{c5}L^{(o)}_{r,11}\right)}{D^{(2)}_{tr}} & n\dfrac{L^{(o)}_{r,21}f_{c7}}{D^{(2)}_{tr}} & \dfrac{-f_{c1}L^{(o)}_{r,11}}{D^{(2)}_{tr}} \end{bmatrix}$$

and

$$D^{(1)}_{tr} = \det\left[L^{(i)}_{r,ij}\right]$$

$$D^{(2)}_{tr} = \det\left[L^{(o)}_{r,ij}\right]$$

Finally, matching of the displacements and slope of the shell at the boundary where the ring is attached, with the displacements and rotation of the ring leads to the following relations:

$$
\begin{Bmatrix} w_{rn} \\ u_{rn} \\ v_{rn} \\ \beta_{rn} \end{Bmatrix} = [M_{T,ij}] \begin{Bmatrix} w_n(\ell/2) \\ u_n(\ell/2) \\ v_n(\ell/2) \\ w'_n(\ell/2) \end{Bmatrix}
$$ (D-4)

with

$$
[M_{T,ij}] = \begin{bmatrix} \tilde{a} & 0 & 0 & \dfrac{\tilde{d}\,\tilde{h}^2}{2\,(a/h)} \\[2ex] 0 & \tilde{a} & 0 & -\dfrac{\tilde{h}_e \tilde{h}}{(a/h)} \\[2ex] -\dfrac{n\tilde{h}_e \tilde{h}}{(a/h)} & 0 & -\dfrac{\tilde{h}_e \tilde{h}}{(a/h)} + 1 & 0 \\[2ex] 0 & 0 & 0 & -1 \end{bmatrix}
$$

$$i,j = 1 \text{ to } 4$$

The nondimensional ring parameters in the above matrix are given in Table D-1. These parameters correspond to a symmetric H-section that is attached in the interior of the shell (see Fig. 5a). Similar relations exist for the other sections considered. Combining Eqs. (D-3) and (D-4) leads to four homogeneous boundary conditions relating the displacements and slope of the shell at the boundary of the ring, to the nondimensional stress and moment resultants of the shell at the same end:

$$
[M_{T,ij}] \begin{Bmatrix} w_n(\ell/2) \\ u_n(\ell/2) \\ v_n(\ell/2) \\ w'_n(\ell/2) \end{Bmatrix} = [M_{d,ij}] \begin{Bmatrix} \tilde{q}_{xx}(\ell/2) \\ \tilde{n}_{xx}(\ell/2) \\ \tilde{n}_{x\theta}(\ell/2) \\ \tilde{m}_{xx}(\ell/2) \end{Bmatrix},
$$

$$i,j = 1 \text{ to } 4$$

(D-5)

Appendix E

Simplicity of the Eigenvalues for the Linear Dynamic Shell Equations

It is proved in this Appendix E that for fixed values of the circumferential wave number n, there exists only one independent eigenfunction for each eigenfrequency $\tilde{\omega}$ for all admissible homogeneous natural boundary conditions.

Proof:

We will first show that the problem

$$L[X] = 0 \qquad \text{(E-1a)}$$

$$U[X] = 0 \qquad \text{(E-1b)}$$

$$U[X] = [h_{ij}] \begin{Bmatrix} X(0) \\ X'(0) \\ . \\ . \\ . \\ X^{(n_d-1)}(0) \end{Bmatrix} + [g_{ij}] \begin{Bmatrix} X(\ell) \\ X'(\ell) \\ . \\ . \\ . \\ X^{(n_d-1)}(\ell) \end{Bmatrix}$$

$$\text{(E-1c)}$$

with

$$i, j = 1 \text{ to } n_d$$

$$h_{ij} = 0 \text{ for } i > \frac{n_d}{2} \text{ and all } j$$

$$g_{ij} = 0 \text{ for } i < \frac{n_d}{2} \text{ and all } j$$

$$\det[[h_{ij}] + [g_{ij}]] \neq 0$$

has only one independent solution if and only if the corresponding eigenmatrix

$$\mathscr{E} = U[\widetilde{\Phi}] \qquad \text{(E-2)}$$

has rank $(n_d - 1)$, where n_d is the order of the homogeneous ordinary differential Eq. (E-1a) and $\widetilde{\Phi}$ is the Wronskian formed by the foundamental set of independent solutions corresponding to Eq. (E-1a). $U[X]$ is a concise form of the homogeneous boundary conditions imposed on Eq. (E-1a) and is often referred to as *the vector boundary form*.

Let

$$\phi_1(x), \phi_2(x), \cdots, \phi_{n_d}(x) \qquad \text{(E-3)}$$

be the n_d linearly independent solutions forming the fundamental set for Eq. (E-1a), then

$$X = \sum_{i=1}^{n_d} C_i \phi_i(x) \qquad \text{(E-4)}$$

Substituting Eq. (E-4) into Eq. (E-1c), we get

$$U[\widetilde{\Phi}] \begin{Bmatrix} C_1 \\ C_2 \\ . \\ . \\ C_{n_d} \end{Bmatrix} = 0 \qquad \text{(E-5)}$$

with

$$\widetilde{\Phi} = \begin{bmatrix} \phi_1 & \phi_2 & \cdots & \phi_{n_d} \\ \phi_1' & \phi_2' & \cdots & \phi_{n_d}' \\ . & . & \cdots & . \\ \phi_1^{(n_d-1)} & & \cdots & \phi_{n_d}^{(n_d-1)} \end{bmatrix}$$

Equation (E-5) has a nontrivial solution if and only if

$$\det[\mathscr{E}] = \det[U[\widetilde{\Phi}]] = 0 \qquad \text{(E-6)}$$

If the rank of $\mathscr{E}$ is $(n_d - 1)$, this will imply that Eq. (E-1) has only one linearly independent solution. This is based on the theorem which states that Eq. (E-1) has exactly k $(0 \leq k \leq n_d)$ linearly independent solutions if and only if the corresponding vector boundary form $\mathscr{E}$ has rank $(n_d - k)$, where n_d is the order of $L[X]$ (see Ref. 11, p. 291).

We now proceed in applying the above result to the linear eigenvalue problem for a cylindrical shell. For $\tilde{\omega} = \tilde{\omega}_{LF}$ and $n \geq 2$, the resulting characteristic equation is given by

$$C_n(1)\tilde{\lambda}_{nj*}^4 + C_n(2)\tilde{\lambda}_{nj*}^3 + C_n(3)\tilde{\lambda}_{nj*}^2$$
$$+ C_n(4)\tilde{\lambda}_{nj*} + C_n(5) = 0 \qquad \text{(E-7)}$$

where $\tilde{\lambda}_{nj*} = \lambda_{nj}^2$. The above coefficients $C_n(k)$ are given in Appendix C: $j^* = 1$ to 4 and $j = 1$ to 8.

From Ref. 8 we know that for $\tilde{\omega} = \tilde{\omega}_{LF}$ and $n \geq 2$:

$$1 > \tilde{\omega}^2 > r^2 n^4 \simeq (\tilde{\omega}^2)_{\text{ring}} \qquad \text{(E-8)}$$

The bounds on $\tilde{\omega}_{LF}$ in Eq. (E-8) require that for positive λ, we must have

$$C_n(1) \rightarrow (+), C_n(2) \rightarrow (-), C_n(3) \rightarrow (+),$$

$$C_n(4) \rightarrow (\pm), C_n(5) \rightarrow (-)$$

We see that the number of sign alternations in the $C_n(k)$ is three implying that Eq. (E-7) has either three or one positive real root. Similarly one can show that Eq. (E-7) has at most one negative real root. For the above range of $\tilde{\omega}$ and n, Eq. (E-7) has one complex pair of roots thus

deleting the possibility of three real positive roots. The form of λ_{nj} is then:

$$\lambda_{n1,2} = \pm\,\alpha_1,\ \lambda_{n3,4} = \pm\,i\alpha_2,\ \lambda_{n5,6,7,8} = \pm\,(\alpha_3 \pm i\alpha_4)$$

(E-9)

The roots in Eq. (E-9) are distinct, leading to a fundamental set of eight distinct and independent solutions. This result implies that the eigenmatrix columns will be linearly independent. And since the eigendeterminant itself must vanish for a nontrivial solution to exist, thus the largest submatrix with nonvanishing determinant will be a seven-by-seven. We conclude that the eigenmatrix has rank seven and thus there exists only one linearly independent eigenfunction for each eigenfrequency.

Nomenclature

A_r area of ring cross section

a shell mean radius

a_r ring mean radius

$\tilde{a} = \dfrac{a_r}{a}$ mean radii ratio

$D = \dfrac{Eh^3}{12(1-\nu^2)}$ shell flexural rigidity

E Young's modulus of elasticity

G_r, G_r', H_r moment resultants of ring

h shell thickness

h_r ring thickness

I_{xx}, I_{yy}, I_p principal moments of inertia of ring cross section

J_{eff} effective moment of inertia in torsion

$k_{xx}, k_{\theta\theta}, k_{x\theta}$ nondimensional change of curvature of shell

ℓ^* shell length

$\ell = \dfrac{\ell^*}{a}$ nondimensional shell length

$m_{xx}, m_{\theta\theta}, m_{x\theta}$ shell nondimensional moment resultants

N_r, N_r', T_r stress resultants of ring

$n_{xx}, n_{\theta\theta}, n_{x\theta}, n_{\theta x}$ shell nondimensional normal stress resultants

m number of half axial waves

n number of circumferential full waves

$q_{xx}, q_{\theta\theta}$ shell nondimensional shear resultants

$r = \dfrac{h}{(12)^{1/2}\, a}$ nondimensional radius of gyration of shell cross section

$r_x = \dfrac{1}{a_r}\left(\dfrac{I_{xx}}{A_r}\right)^{1/2}$ nondimensional out-of-plane radius of gyration of ring cross section

$r_y = \dfrac{1}{a_r}\left(\dfrac{I_{yy}}{A_r}\right)^{1/2}$ nondimensional in-plane radius of gyration of ring cross section

$r_p = \dfrac{1}{a_r}\left(\dfrac{I_p}{A_r}\right)^{1/2}$ nondimensional polar radius of gyration of ring cross section

$r_t = \dfrac{1}{a_r}\left(\dfrac{J_{eff}}{A_r}\right)^{1/2}$ nondimensional radius of gyration in torsion of ring cross section

$S_{tx} = \dfrac{r_x}{r}\,(W_r\tilde{a})^{1/2}$ out-of-plane ring stiffness factor

$S_{ty} = \dfrac{r_y}{r}\,(W_r\tilde{a})^{1/2}$ in-plane ring stiffness factor

Nomenclature (contd)

$s = \dfrac{m\pi}{\ell}$ nondimensional axial wave length parameter

t time

u^*, v^*, w^* shell displacements

$u = \dfrac{u^*}{a}, v = \dfrac{v^*}{a}, w = \dfrac{w^*}{a}$ nondimensional shell displacements

$u_r^*, v_r^*, w_r^*, \beta_r$ ring displacements and rotation about its center line (Z axis of ring)

$u_r = \dfrac{u_r^*}{a_r}, v_r = \dfrac{v_r^*}{a_r}, w_r = \dfrac{w_r^*}{a_r}$ nondimensional ring displacements

W_r weight ratio (weight of ring/weight of shell)

X, Y, Z orthogonal coordinate system for ring

x^* running coordinate in axial direction for shell

$x = \dfrac{x^*}{a}$ nondimensional axial running coordinate

β_r rotation of ring cross section about its center line

$\epsilon_{xx}, \epsilon_{\theta\theta}, \epsilon_{x\theta}$ membrane strains of shell

θ running coordinate in circumferential direction

ν Poisson's ratio

ρ density of shell material

$\tau = \omega_o t$ Nondimensional time

$\omega_o = \left[\dfrac{E}{\rho a^2 (1 - \nu^2)} \right]^{1/2}$ axisymmetric ring frequency

$\tilde{\omega} = \dfrac{\omega}{\omega_o}$ nondimensional frequency

References

1. Gros, C., and Forsberg, K., *Vibrations of Shells, a Partially Annotated Bibliography,* SB 63-43. Lockheed Missile and Space Corp. Sunnyvale, Calif., 1963.

2. Arnold, R., and Warburton, G., "Flexural Vibrations of Walls of Thin Cylindrical Shells Having Freely Supported Ends." *Proc. Roy. Soc. London, Ser. A,* Vol. A197, pp. 238-256, 1949.

3. Arnold, R.. and Warburton, G., "The Flexural Vibrations of Thin Cylinders," *Inst. Mech. Eng. London Proc., Ser. A, Auto. Div.,* Vol. 167, 1953, pp. 62-64 and 74-80, 1953.

4. Weingarten, V., *On the Free Vibrations of Thin Cylindrical Shells,* TDR 169 (3560-30) TN-3, SSD TDR-63-6, Aerospace Corp. Systems Research and Planning Div., Dec. 1962.

5. Forsberg, K., "Influence of Boundary Conditions on the Modal Characteristics of Thin Cylindrical Shells," *AIAA J.,* Vol. 2, No. 12, 1964.

6. Forsberg, K., Axially Symmetric and Beam Type Vibrations of Thin Cylindrical Shells, AIAA Paper 66-447. *4th Aerospace Sciences Meeting,* Los Angeles, Calif., June 1966.

7. Cohen, G., "Buckling of Axially Compressed Cylindrical Shells With Ring-Stiffened Edges," *AIAA J.,* Technical Note, p. 1858, Oct. 1966.

8. El Raheb, M., *Some Approximations in the Dynamic Shell Equations.* Ph.D. Thesis, Dept. of Aeronautics, California Institute of Technology, Pasadena, Calif., Dec. 1969.

9. Forsberg, K., Brogan, F., and Smith, S., Dynamic Behavior of a Cylinder With a Cutout. *AIAA J.,* Vol. 7, No. 5, May 1969.

10. Love, A., *Mathematical Theory of Elasticity.* Dover Publications, New York, 1944.

11. Coddington, E., and Levinson, N., *Theory of Ordinary Differential Equations.* McGraw-Hill Book Co., New York, 1955.

12. Arbocz, J., and Babcock, C. D., "The Effect of General Imperfections on the Buckling of Cylindrical Shells," *J. Appl. Mech.,* Mar. 1969.

1. Report No. 32-1489	2. Government Accession No.	3. Recipient's Catalog No.

4. Title and Subtitle	5. Report Date March 1, 1971
EFFECT OF ELASTIC END RINGS ON THE EIGEN-FREQUENCIES OF FINITE LENGTH THIN CYLINDRICAL SHELLS	6. Performing Organization Code

7. Author(s) Michel El Raheb	8. Performing Organization Report No.

9. Performing Organization Name and Address	10. Work Unit No.
JET PROPULSION LABORATORY California Institute of Technology 4800 Oak Grove Drive Pasadena, California 91103	11. Contract or Grant No. NAS 7-100
	13. Type of Report and Period Covered Technical Report

12. Sponsoring Agency Name and Address	
NATIONAL AERONAUTICS AND SPACE ADMINISTRATION Washington, D.C. 20546	14. Sponsoring Agency Code

15. Supplementary Notes

16. Abstract

The effect of elastic end rings on the eigenfrequencies of thin cylindrical shells was studied by using an exact solution of the linear eigenvalue problem. The in-plane boundary conditions which proved to be very influential in the neighborhood of the minimum frequency were exactly satisfied. The out-of-plane and torsional rigidities of the ring were found to govern the overall shell stiffness. Considerable mode interaction was noticed at low circumferential wave numbers for low values of the ring stiffness.

Rings were closed section were found to be more efficient than those with open section for the same values of weight ratio. No appreciable difference was noticed between rings fixed from the inside or the outside of the shell mid-surface.

17. Key Words (Selected by Author(s))	18. Distribution Statement
Mathematical Sciences Mechanics Solid-State Physics Structural Engineering	Unclassified -- Unlimited

19. Security Classif. (of this report)	20. Security Classif. (of this page)	21. No. of Pages	22. Price
Unclassified	Unclassified	26	